

## ANALYSIS OF THE QUIESCENT LOW-MASS X-RAY BINARY POPULATION IN GALACTIC GLOBULAR CLUSTERS

C. O. HEINKE<sup>1</sup>, J. E. GRINDLAY<sup>1</sup>, P. M. LUGGER<sup>2</sup>, H. N. COHN<sup>2</sup>, P. D. EDMONDS<sup>1</sup>, D. A. LLOYD<sup>1</sup>, AND A. M. COOL<sup>3</sup>*Submitted to ApJ*

## ABSTRACT

Quiescent low-mass X-ray binaries (qLMXBs) containing neutron stars have been identified in several globular clusters using *Chandra* or XMM X-ray observations, using their soft thermal spectra. We report a complete census of the qLMXB population in these clusters, identifying three additional probable qLMXBs in NGC 6440. We conduct several analyses of the qLMXB population, and compare it with the harder, primarily CV, population of low-luminosity X-ray sources with  $10^{31} < L_X < 10^{32.5}$  ergs s<sup>-1</sup>. The radial distribution of our qLMXB sample suggests an average system mass of  $1.5_{-0.2}^{+0.3} M_{\odot}$ , consistent with a neutron star and low-mass companion. Spectral analysis reveals that no globular cluster qLMXBs, other than the transient in NGC 6440, require an additional hard power-law component as often observed in field qLMXBs. We identify an empirical lower luminosity limit of  $10^{32}$  ergs s<sup>-1</sup> among globular cluster qLMXBs. The bolometric luminosity range of qLMXBs implies (in the deep crustal heating model of Brown and collaborators) low time-averaged mass transfer rates, below the disk stability criterion. The X-ray luminosity functions of the CV populations alone in NGC 6397 and 47 Tuc are shown to differ. The distribution of qLMXBs among globular clusters is consistent with their dynamical formation by either tidal capture or exchange encounters, allowing us to estimate that seven times more qLMXBs than bright LMXBs reside in globular clusters. The distribution of harder sources (primarily CVs) has a weaker dependence upon density than that of the qLMXBs. Finally, we discuss possible effects of core collapse and globular cluster destruction upon X-ray source populations.

*Subject headings:* X-rays : binaries — novae, cataclysmic variables — globular clusters: general — globular clusters: individual (NGC 6440) — stars: neutron — stellar dynamics

## 1. INTRODUCTION

Globular clusters have proven to be an excellent place to study accreting binary systems, due to their known distances, ages, and reddening which allow system parameters and histories to be better understood than in the field. It has long been suspected that globular clusters may also provide unique channels for the formation of accreting binaries, starting with the discovery that low-mass X-ray binaries (LMXBs) are  $\sim 100\times$  more common (per unit mass) in globular clusters than in the field (Clark 1975; Katz 1975). It is now thought that X-ray binary systems in dense globular clusters are created principally through exchange interactions between primordial binaries and other stars (see, e.g. Hut, Murphy & Verbunt 1991). Therefore, studying accreting binary systems in globular clusters can give us insight into the characteristics of accreting binary systems and populations, and also into dynamical effects inside globular clusters.

The giant leap forward in sensitivity and resolution offered by the *Chandra* X-ray Observatory, especially when combined with the unparalleled resolution of the *Hubble Space Telescope* (*HST*), has revolutionized our understanding of globular clusters. Prior to *Chandra*, there were 12 bright cluster LMXBs (now 13, all thought to have neutron stars [NS] as primaries), and 57 faint X-ray sources known in the Galactic globular cluster system (Verbunt 2001). A few of the latter had been identified with cat-

aclysmic variables (CVs; Hertz & Grindlay 1983, Cool et al. 1995, Grindlay et al. 1995), and some were thought to be LMXBs in quiescence (qLMXBs; Verbunt, Elson & van Paradijs 1984), but their properties were poorly understood due to the poor spatial and/or spectral resolution of previous X-ray observatories. *Chandra* has identified more than 100 X-ray sources in the globular cluster 47 Tuc alone (Grindlay et al. 2001a, hereafter GHE01a). Dozens of sources have been discovered in the globular clusters  $\omega$  Cen (Rutledge et al. 2002a, Cool, Haggard, & Carlin 2002), NGC 6397 (Grindlay et al. 2001b, hereafter GHE01b), NGC 6752 (Pooley et al. 2002a), NGC 6440 (Pooley et al. 2002b; in't Zand et al. 2001), M28 (Becker et al. 2003), Terzan 5 (Heinke et al. 2003b), and M80 (Heinke et al. 2003c). These plus preliminary results from several additional clusters create a sizable dataset for comparison of X-ray source populations with cluster properties (Pooley et al. 2003a, b), especially when combined with initial XMM results on the low-density clusters M22,  $\omega$  Cen, and M13 (Webb, Gendre & Barret 2002; Gendre et al. 2003a, b). *HST* identifications have allowed the classification of many as CVs or active main-sequence or subgiant binaries (ABs) in 47 Tuc (Edmonds et al. 2003a,b), NGC 6397 (GHE01b), NGC 6752 (Pooley et al. 2002a), and  $\omega$  Cen (Cool, Haggard, & Carlin 2002), and one as a qLMXB in 47 Tuc (Edmonds et al. 2002a). Radio-derived positions or orbital periods for millisecond pulsars (MSPs) have al-

<sup>1</sup> Harvard-Smithsonian Center for Astrophysics, 60 Garden Street, Cambridge, MA 02138; cheinke@cfa.harvard.edu, josh@cfa.harvard.edu, pedmonds@cfa.harvard.edu, dlloyd@cfa.harvard.edu

<sup>2</sup> Department of Astronomy, Indiana University, Swain West 319, Bloomington, IN 47405; lugger@indiana.edu, cohn@indiana.edu

<sup>3</sup> San Francisco State U., 1600 Holloway Ave. San Francisco, CA 94132; cool@quark.sfsu.edu

lowed the identification of faint X-ray sources as MSPs in 47 Tuc (Edmonds et al. 2001; Grindlay et al. 2002; Edmonds et al. 2002b), NGC 6397 (GHE01b), and NGC 6752 (D’Amico et al. 2002). However, radio and *HST* coverage of globular clusters is generally quite incomplete, and faint X-ray sources in most globular clusters do not have clear identifications from other wavebands. Even with deep radio and optical data, MSPs may be confused with CVs (see Edmonds et al. 2002b) or with ABs (Ferraro et al. 2001, but cf. Edmonds et al. 2003b). However, qLMXBs show clear differences from all other types of globular cluster X-ray sources in their colors and luminosities ( $L_X \sim 10^{32-34}$  ergs s<sup>-1</sup>, with soft X-ray colors) and detailed spectra (a thermal component with implied radius of a few km, sometimes accompanied by a nonthermal harder component). Their X-ray emission is thought to be due principally to thermal emission from the neutron star surface (Brown, Bildsten, & Rutledge 1998; Campana et al. 1998), thus making their X-ray signatures more homogeneous than X-rays from other source types. These differences make it practical to identify a homogeneous sample of qLMXBs in different globular clusters without the need for deep *HST* or radio datasets, using X-ray spectra, colors, and luminosities alone, as for instance in 47 Tuc (GHE01a),  $\omega$  Cen (Rutledge et al. 2002a), NGC 6397 (GHE01b), NGC 6440 (Pooley et al. 2002b), and M28 (Becker et al. 2003).

We perform several analyses of the qLMXB population that has been uncovered in numerous globular clusters. The qLMXB population in globular clusters offers hope for understanding many questions related to neutron stars, accretion flows, and cluster dynamics. Among these questions: what is the source of the X-ray luminosity observed from qLMXBs, deep crustal heating (Brown et al. 1998) or continued low-level accretion? What is the nature and origin of the nonthermal hard component observed in many qLMXB spectra? How long are qLMXBs in quiescence between outbursts? Are qLMXBs part of the progenitor population of MSPs? Can we constrain the radius and/or mass of qLMXBs through observation of the thermal component of their spectra? What are the parameters of globular clusters that cause the formation of qLMXBs? Can their numbers be fully explained through two-body or single-binary encounter rates? Are other globular cluster X-ray sources (such as CVs) formed in the same way? We will gather evidence to begin answering these questions in this paper.

In §2 we identify a sample of confirmed and potential qLMXBs containing neutron stars in several globular clusters, and analyze their X-ray spectra. In §3.1 we study the qLMXB radial distributions in King-model clusters. In §3.2 we analyze the qLMXB (and harder sources) luminosity functions, while in §3.3 we analyze the dependencies of qLMXB and harder source numbers upon cluster structural parameters. In §4 we discuss the meaning of qLMXB radial distributions and spectra (§4.1), qLMXB luminosities (§4.2), qLMXB vs. CV distributions among clusters (§4.3), and additional dynamical processes (§4.4). Finally we summarize in §5.

## 2. QUIESCENT LMXBS

Identifying the nature of X-ray sources is often difficult, requiring deep multiwavelength data. The unique X-ray

spectral signature of a qLMXB, however, offers the possibility of identifying qLMXBs without multiwavelength followup (important since they can be extremely optically faint; see Edmonds et al. 2002a, GHE01b). In the field, qLMXBs containing neutron stars have been identified after bright transient outbursts, often exhibiting type I X-ray bursts confirming their neutron star nature. (See Campana et al. 1998 for a review.) Their quiescent spectra show a thermal component roughly consistent with a 10 km neutron star (when hydrogen atmospheres are taken into account, e.g. Brown et al. 1998). In addition, a harder component parametrized as a power-law of photon index 1 to 2 is often seen, comprising up to 40% of the 0.5-10 keV emission (Campana et al. 1998; Rutledge et al. 2002b and refs therein). Their minimum X-ray (0.5-2.5 keV) luminosity appears to range between  $5 \times 10^{31}$  and a few  $10^{33}$  ergs s<sup>-1</sup>, although distances and thus luminosities are uncertain. Comparison with field systems has thus allowed numerous qLMXBs to be identified in X-ray studies of globular clusters (see below).

The large sample of qLMXBs now known in several globular clusters allows significant comparative study. The known distances and reddening to globular clusters allows accurate luminosities to be derived, generally impossible in the field. We can fit the spectra to look for a hard power-law component as seen in some field qLMXBs, and to check for consistency with a 10 km, 1.4  $M_\odot$  neutron star explanation. Calibration changes since the publication of some early papers makes revisiting the spectral analysis on several clusters desirable, while a common standard for identifying qLMXBs would also be useful. For all analysis in this paper, we use photoelectric absorption X-ray cross-sections of Balucinska-Church & McCammon (1992) in the XSPEC *phabs* model.

For this paper we choose to identify a “canonical” qLMXB signature, spectral consistency with a nonmagnetic hydrogen atmosphere of implied radius  $\sim 10$  km, with a small ( $< 40\%$  of 0.5-10 keV flux) contribution from a power-law component allowed. This is chosen to match qLMXB systems studied in the field (Cen X-4, Rutledge et al. 2001; Aql X-1, Rutledge et al. 2002b; 4U 2129+47, Nowak et al. 2002), and gives a spectrum much softer than that from known CVs. A notable exception to this signature is the millisecond X-ray pulsar SAX J1808.4-3658 (SAX J1808), which has shown an extremely faint ( $L_X(0.5-10 \text{ keV}) = 5 \times 10^{31} \text{ erg s}^{-1}$ ) quiescent spectrum in a recent XMM observation dominated by a hard (photon index  $\sim 1.5$ ) power-law component (Campana et al. 2002). We would not be able to distinguish such an object from CVs with similar spectra in globular clusters. Therefore we concentrate in this paper on studying a sample of objects which we can be fairly certain are qLMXBs.

As a comparison sample, we discuss spectrally harder objects of similar X-ray luminosity. Based on optical analysis in several clusters (GHE01a, GHE01b, Pooley et al. 2002a, Edmonds et al. 2003a), these are thought to be mostly CVs, at least above  $10^{31} \text{ erg s}^{-1}$  (below which active binaries and MSPs become numerous). One hard X-ray source at the upper end of this luminosity range has been identified as a bright MSP in the globular cluster M28 (Becker et al. 2003), while a moderately hard source in 47 Tuc with an unusual spectrum and strong variability

has been suggested as a qLMXB (X10; GHE01a, Edmonds et al. 2003b). Transient black holes in quiescence have X-ray spectra and luminosities indistinguishable from those of CVs, although none have yet been positively identified in a globular cluster. The great majority of these hard objects are probably CVs, as we show below.

CVs, composed of a (usually low-mass main-sequence) secondary, a white dwarf, and an accretion disk, display several optical signatures. In  $U$  vs.  $U - V$  CMDs they appear bluer than the main sequence, usually lying between the main sequence and the white dwarf cooling sequence. A strong contributor to this blue color, the accretion disk, will also generate H- $\alpha$  emission, and cause short-timescale nonperiodic variability (flickering) and sometimes large-amplitude outbursts. In  $V$  vs.  $V - I$  CMDs, CVs generally appear redder due to the increased contribution of the secondary light, and in globular clusters have often been observed to fall on or near the main sequence (Edmonds et al. 2003a). The secondary, filling its Roche lobe, will often show ellipsoidal variations, and this periodic, low amplitude signal is detectable if the noise from flickering is not too large. The X-ray to optical flux ratio for CVs should be smaller than for qLMXBs, and a CV at a given X-ray luminosity will display much bluer colors than a qLMXB at the same luminosity, since it must be accreting at a much higher rate. Based on these characteristics, X-ray sources can be identified as CVs with high confidence.

Detailed searches for variability and/or H- $\alpha$  excess among blue counterparts to *Chandra* X-ray sources have been published for three clusters, NGC 6397, NGC 6752, and 47 Tuc. Six CVs have been optically identified among 8 hard X-ray sources with  $L_X(0.5 - 2.5) > 10^{31}$  ergs s $^{-1}$  in NGC 6397 (GHE01b). The two unidentified objects are an active binary system and a probable CV (based on an  $N_H$  column above the cluster value). Similarly, six CVs have been optically identified in NGC 6752 (Pooley et al. 2002a) among 8 hard cluster sources with  $L_X(0.5 - 2.5) > 10^{31}$  ergs s $^{-1}$ , including one probable BY Dra system and one unidentified source. (See §2.5 for discussion of the soft source CX8 in NGC 6752.) Finally, 12 CVs have been identified among 18 hard sources with  $L_X(0.5 - 2.5) > 10^{31}$  ergs s $^{-1}$  in 47 Tuc (GHE01a, Edmonds et al. 2003a, b). The other six include three active binary systems and three sources with marginal optical counterparts that are suggested as CVs. Thus the fraction of non-CVs among this population seems to be less than  $\sim 20\%$  in three very different clusters.

Quiescent LMXBs have been spectrally identified in 47 Tuc (2; GHE01a),  $\omega$  Cen (1; Rutledge et al. 2002a), NGC 6397 (1; GHE01b), NGC 6440 (4-5; Pooley et al. 2002b, in't Zand et al. 2001), M28 (1; Becker et al. 2003), Terzan 5 (4 plus the transient LMXB; Heinke et al. 2003b), M13 (1; Gendre et al. 2003b), M30 (1; Lugger et al. 2003), M80 (2; Heinke et al. 2003c), and NGC 6266 (5; Pooley et al. in prep.). Spectral analyses have been performed for most of these. However, in several cases the work was performed before the low-energy *Chandra* quantum efficiency degradation was known and calibrated, so we repeat the analysis. We also attempt a census of all qLMXBs in clusters studied with *Chandra* or XMM. We summarize some important quantities, and results from *Chandra* or XMM

studies of several clusters, in Table 1 (with clusters listed in order of decreasing close encounter rates, see §3.3 and §4.3). Physical quantities are from the catalog of Harris 1996, updated 2003<sup>4</sup>, with a few additional updates, principally core radii and distances (referenced).

### 2.1. 47 Tuc & M30

These clusters have been recently analyzed (Heinke et al. 2003a, Lugger et al. 2003) with the same nonmagnetic hydrogen-atmosphere model (Lloyd 2003) used in this work. We include the relevant results from their analyses of these qLMXBs in Table 2. We correct the luminosities and radii for the fraction of the 1 keV *Chandra* point spread function included in the extraction circles, using the CIAO tool *mkpsf*. The luminosity corrections amount to factors of 1.05 and 1.10 for 47 Tuc and M30 respectively; this small correction was not applied to the 47 Tuc results in Heinke et al. (2003a). The possibility that X10 in 47 Tuc may be a qLMXB was suggested by Edmonds et al. (2003b) on the basis of its high X-ray to optical flux ratio. However, this object is dramatically variable in the X-ray (GHE01a), while the X-ray and optical flux measurements were not simultaneous (as pointed out by Edmonds et al. 2003b). Its X-ray spectrum can be described as a power-law of photon index 3, with no apparent contribution from a thermal hydrogen atmosphere component (GHE01a). We also note that the optical counterpart V3, while on the main sequence in a  $V$ ,  $V - I$  CMD, falls near the white dwarf cooling tracks 2.8 magnitudes bluewards of the main sequence in a  $U$ ,  $U - V$  CMD (Edmonds et al. 2003a). This indicates a very strong contribution of U light from the disk, similar to several other CVs apparent in the 47 Tuc CMDs of Edmonds et al. (2003a). This can be compared to the known qLMXB X5, which falls roughly 0.9 magnitudes bluewards of the main sequence in a F300W, F300W-F555W CMD (Edmonds et al. 2003a). The difference in  $U$  contributions suggests that significantly more mass transfer is occurring in X10 than X5. X5's high inclination could reduce its disk component, but the eclipsing CVs W8 and W15 also appear very blue (Edmonds et al. 2003a). Further investigation of the X-ray and optical properties of this object in the coordinated simultaneous *Chandra/HST* observations of 47 Tuc in late 2002 is underway, and should resolve the question of X10's nature. For the purposes of this paper, we simply note that X10 does not fit our "canonical" qLMXB definition above, and so we exclude it from our qLMXB analysis.

### 2.2. M28 & M13

Quiescent LMXBs in these clusters have been recently analyzed using the Zavlin, Pavlov, & Shibanov (1996) nonmagnetic hydrogen atmosphere *nsa* model (Becker et al. 2003, Gendre et al. 2003b). This model gives very similar results to the Lloyd (2003) model. Since the data are not yet public, we include the results of their analyses in our table. Since we are quoting true radii and  $T_{eff}$  rather than  $R^\infty$  and  $T_{eff}^\infty$ , we calculate the temperature and radius results using the assumption of  $z=0.306$ . The luminosity values given in Gendre et al. (2003b) and Becker et al. (2002) are not for the same energy ranges as our

<sup>4</sup> Available at <http://physun.physics.mcmaster.ca/Globular.html>

0.5-2.5 keV range. We used the Zavlin et al. (1996) *nsa* model, with the same temperatures and radii as the best fits in these papers, to calculate the ratios of unabsorbed flux in our energy bands to their energy bands, and thus generated the luminosities in Table 2.

### 2.3. $\omega$ Cen, NGC 6397, Terzan 5, and M80

For these clusters we re-extract source and background spectra of qLMXB candidates in the same way as in the original works (Rutledge et al. 2002a, GHE01b, Heinke et al. 2003b, Heinke et al. 2003c), except that we use an extraction circle of 2" for NGC 6397 U24. We calculate the fraction of the 1 keV *Chandra* point-spread function that is included in each region using the CIAO tool *mkpsf*. We applied a correction to the effective area functions to account for degradation of low-energy quantum efficiency. We group the channels to ensure  $\geq 20$  counts per bin, and fit the data in XSPEC (Arnaud 1996). For M80 CX6 (only 62 counts), we do not group the channels, and instead use the C statistic for analysis. This would be preferable for the faint sources in Terzan 5, but the background is extremely high due to the outburst by the transient LMXB. When we use the C statistic, we test the fit by generating Monte Carlo simulations of the best fit spectrum. Roughly half the Monte Carlo simulations should show lower values of the C statistic than the data, if the fit is good. The percentage of simulations showing a lower C statistic than the best fit is shown in Table 2 for sources where we use the C statistic.

For each qLMXB we fit a model consisting of photoelectric absorption fixed at the cluster value and the nonmagnetic hydrogen atmosphere of Lloyd (2003), plus an optional power-law component. The power-law component in field systems has been observed with a photon index ranging from 1 to 2, and contributing up to 40% of the flux (see Rutledge et al. 2002b; but cf. Campana et al. 2002 on SAX J1808). To simplify our analysis and allow direct comparison between objects, we fix the photon index of the possible power-law component at 1.5. The results of these fits are shown in Table 2. Luminosities are increased to account for aperture corrections by factors of 1.10 for Terzan 5, 1.02 for  $\omega$  Cen, 1.03 for NGC 6397, and 1.07 for M80; derived radii are adjusted accordingly. All spectral errors, but not luminosity errors, are given at 90% confidence for a single parameter using the XSPEC *error* command. For power-law component upper limits, this translates to 95% confidence. We note that this procedure may significantly underestimate strongly covariant uncertainties, such as radius and temperature, especially when the absorption is large (see in't Zand et al. 2001). Therefore we offer radius estimates as a consistency check, and not as a serious attempt as a constraint upon the radii of these objects, especially for small numbers of counts. This is especially true since we have not considered intrinsic absorption in these systems. The values for Terzan 5 are especially questionable due to the extremely high background; for W4 we make no attempt to constrain any power-law component (although none is required). We include these parameters for completeness and to generate luminosities. Upcoming *Chandra* observations of Terzan 5 in July 2003 (principal investigator: R. Wijnands) should allow much better constraints upon these sources if the

transient remains in quiescence as expected.

### 2.4. NGC 6440

For NGC 6440 we downloaded the data from the archive and removed the pixel randomization applied in standard processing. Then we extracted spectra from 1"2 radius circles around *wavdetect*-identified locations of the softer sources (CX1, CX2, CX3, CX5, CX7, CX8, CX10, CX11, CX12, CX13) from Pooley et al. (2002b), except where severe crowding reduced our region size (to 0"86 for CX11). We grouped counts to 20 per bin to ensure  $\chi^2$  statistic applicability except when the source had fewer than 100 counts, where we left the data unbinned and used the C statistic in XSPEC for analysis (as above). We fix the absorption to the cluster value of  $0.59 \times 10^{22} \text{ cm}^{-2}$  (as in Pooley et al. 2002b) for all sources. We demand that candidate qLMXBs be acceptably fit with a hydrogen atmosphere alone, or require that the power-law component comprise no more than 40% of the 0.5-10 keV flux (see above). All luminosities and radii are adjusted to account for the extraction regions; this amounts to a factor of 1.07 in luminosities for the qLMXBs we identify. In this way, we find several additional qLMXB candidates in NGC 6440.

The quiescent spectrum of the X-ray transient NGC 6440 CX1 was analyzed by in't Zand et al. (2001), who assume a higher  $N_H$  column ( $0.82 \times 10^{22} \text{ cm}^{-2}$ ) than the galactic column to the cluster. They base this upon the agreement between the  $N_H$  columns derived by a 1998 BeppoSAX observation of CX1 in outburst (in't Zand et al. 1999), and their analysis of the spectrum of an annulus around the outbursting transient in a 2001 *Chandra* observation. However, the BeppoSAX spectrum gives different  $N_H$  values depending on the assumed model, and the *Chandra* 2001 annulus spectrum of the outburst will be affected by the energy dependence of the point-spread function. Also, internal absorption is often observed to vary in accreting systems, especially during outbursts. Therefore, we perform our own determination of  $N_H$  for the quiescent spectrum of CX1. When we allow  $N_H$  to float, we find  $N_{H,22} = 0.66_{-10}^{+11}$ . Using the *nsa* model of Zavlin et al. (1996) and forcing the power-law photon index to be 1.44 (as done by in't Zand et al. 2001), but using more recent photoelectric cross-sections, we find  $N_{H,22} = 0.70_{-10}^{+18}$  (and  $R = 9.5_{-1.5}^{+0.7} \text{ km}$ ). We consider the absorption to CX1 to remain uncertain, and quote results assuming the cluster absorption in Table 2.

Our results strongly support the suggestion by Pooley et al. (2002b) that CX2, CX3, CX5, and CX7 are likely qLMXBs. Although the best fits for CX3 and CX5 include a power-law component, this component cannot be considered significantly detected. We also identify three additional possible qLMXBs, CX10, CX12, and CX13. Each of these objects is consistent with a 10 km hydrogen-atmosphere neutron star spectrum, without a power-law component. Their luminosities are also similar to those of known qLMXBs in  $\omega$  Cen (Rutledge et al. 2002a), NGC 6397 (GHE01b), and M80 (CX6; Heinke et al. 2003c). None of these objects show clear variability, though the number of counts from each is low. We include their spectral parameters in Table 2, although we note that their low counts make these parameters individually unreliable.

For the harder objects CX8 and CX11, we can rule out

a hydrogen atmosphere as the primary contribution to the observed flux. For CX8 a 10-km radius hydrogen atmosphere is a bad fit (100 Monte Carlo simulations of the best fit gave uniformly lower values of the C statistic than the data). A hydrogen atmosphere with an additional power-law component is an acceptable fit, but has  $70^{+30}_{-24}\%$  of the unabsorbed 0.5-10 keV flux (92% of the received flux) in the power-law component. For CX11 a 10 km-radius hydrogen atmosphere alone is as bad a fit as for CX8. A hydrogen atmosphere with an additional power-law component is an acceptable fit, but has  $47^{+30}_{-24}\%$  of the unabsorbed 0.5-10 keV flux (83% of the received flux) in the power-law component. Although the uncertainties of the fit allow less than 40% of the unabsorbed flux to be in the power-law component, we think this object is unlikely to be a qLMXB. The remaining sources above CX11's luminosity are too hard to fit our canonical qLMXB model.

Fainter sources in the observation are uniformly harder than our suggested qLMXBs, and have too few counts for even the simplest spectral fitting to be meaningful. We note that CX13 is as faint (or fainter) as the faintest other qLMXBs identified in any globular cluster. Although confusion may have prevented the identification of perhaps one qLMXB, we conclude that this census of the qLMXBs in NGC 6440 is essentially complete. Follow-up observations of NGC 6440 scheduled for July 2003 (principal investigator: R. Wijnands) will allow testing of these results.

Finally, we utilize a simple graphical method to check the similarity of our candidate qLMXBs to other qLMXBs. We place each of the NGC 6440 qLMXB candidates on a standardized X-ray CMD, using our best-fit luminosities and the unreddened colors derived by Pooley et al. (2002b). We also calculate the positions of several other qLMXBs in other clusters on the same diagram. To do this requires compensating for the reddening to different clusters, as well as accounting for the differences between the response of the front-illuminated ACIS-I chips (used for the observations of 47 Tuc, NGC 6397,  $\omega$  Cen, and Terzan 5) and the back-illuminated ACIS-S chip. We used the CIAO PIMMS tool to estimate the difference in observed Xcolor for several spectra between each cluster's actual observation and a hypothetical ACIS-S observation with no reddening (ignoring the loss of low-energy sensitivity over the *Chandra* mission, which has no effect on the spectra above 1 keV). We derive Xcolor offsets of +0.70 for  $\omega$  Cen, +0.49 for 47 Tuc, +0.73 for NGC 6397, and +0.06 for M30 to place their qLMXBs onto a dereddened ACIS-S CMD. The two qLMXBs in 47 Tuc suffer moderate pileup, which distorts their intrinsic Xcolor. To reduce the hardening effect of pileup, we use the Xcolor derived only from the final 2000 47 Tuc observation (4.7 ksec), which used a 1/4 subarray to avoid pileup (receiving 369 and 423 counts for X5 and X7 respectively). However, we note that these objects (and the M30 qLMXB) still suffer pileup at the  $\sim 2\%$  level, which will harden their spectra and is not accounted for. Finally, we plot the theoretical locations in this diagram of hydrogen atmosphere neutron stars of 10 and 12 km radii over a range of temperatures, using the models of Lloyd (2003) with the gravitational redshift fixed to  $z=0.306$ . These are essentially neutron star cooling tracks.

This X-ray CMD (Figure 1) clearly shows agreement be-

tween the theoretical hydrogen atmosphere cooling tracks and the observed locations of identified and candidate qLMXBs. We caution that the apparent close agreement with the 12-km track should not be taken too seriously due to the numerous possible errors listed above. We also plot the theoretical track of a blackbody, with radius arbitrarily set to 1.41 km. A clear difference can be seen between the predictions of a blackbody vs. the hydrogen atmosphere models, with the colors and luminosities of the qLMXBs favoring the hydrogen atmosphere model. This diagram shows the utility of a standardized X-ray CMD, and the importance of hydrogen-atmosphere neutron star models.

## 2.5. Other clusters

Several other clusters have been studied with *Chandra*'s ACIS detector to a depth sufficient to identify any of the qLMXBs above. Pooley et al. (2002a) find no objects in NGC 6752 with luminosities and spectra similar to those found in other clusters. However, they do identify a source (CX8) within the half-mass radius of NGC 6752 which shows an extremely soft spectrum, placing it near the neutron star cooling track in Figure 1, at an implied  $L_X = 2 \times 10^{31}$  ergs/s. We note that no thermally radiating MSP has been identified at these luminosities; from Grindlay et al. (2002), we see that the 0.5-2.5 keV X-ray luminosities of thermally emitting MSPs range from  $1-4 \times 10^{30}$  ergs/s. Nonthermally-emitting MSPs can be brighter (GHE01b, Edmonds et al. 2002b, Becker et al. 2003), but also have much harder spectra. Identification of a thermally emitting neutron star in the "gap" between the tail of the qLMXB luminosity function and the MSP nexus would be of great interest.

We extracted the spectrum of CX8 from the *Chandra* archival observation of NGC 6752, using a 2" extraction region and binning the 83 counts with 10 counts/bin. XSPEC fits with a hydrogen atmosphere model give atrocious fits; fixing the radius to 10 km and the absorption at the cluster value gives  $\chi^2_\nu=7.4$  for 8 degrees of freedom (dof), while allowing the radius to be a free parameter ( $R \sim 0.9$  km) gives  $\chi^2_\nu=2.4$  for 7 dof. The poor quality of these fits is induced by a feature resembling an emission line complex located at  $\sim 0.9$  keV. This indicates an optically thin low-temperature plasma, so we fit an XSPEC MEKAL optically thin plasma model (Liedahl, Osterheld, & Goldstein 1995 and refs therein), deriving  $kT = 0.77 \pm .11$  keV and an iron abundance  $23^{+38}_{-12}\%$  of solar. This iron abundance is inconsistent with the metallicity of NGC 6752,  $[\text{Fe}/\text{H}]=-1.65$  (3% solar), from Harris (1996). The metallicity inconsistency and the large ( $\sim 88''$ , 8.5 core radii) offset of CX8 from the core of NGC 6752 suggest that CX8 may not be a member of the cluster, but rather a foreground star or active binary.

Preliminary analyses of deep *Chandra* or XMM data have been presented for five other clusters at scientific conferences or in other works at the time of writing. According to both Pooley et al. (2003a) and Gendre et al. (2003b), NGC 6366 possesses no qLMXBs. NGC 6121 has no qLMXBs (Bassa et al. in prep.; Pooley et al. 2003a), nor does NGC 5904 (Pooley et al. 2003a). The rich, dense cluster NGC 6266 (Pooley et al. 2003b, Pooley et al. in prep.) has five identified qLMXBs (D. Pooley,

priv. comm.). Reassessment of the XMM data on M22 (Webb et al. 2002) by Gendre et al. (2003b) indicates that no qLMXBs matching our template are present in that cluster. In each case the sensitivity of the observation is sufficient to confidently identify all possible qLMXBs above our empirical lower  $L_X$  limit of  $1 \times 10^{32}$  erg s $^{-1}$ . In most of these clusters the sensitivity is sufficient to identify all harder sources above  $L_X(0.5\text{-}2.5 \text{ keV}) > 10^{31}$  ergs s $^{-1}$  (Pooley et al. 2003a, b; see Table 1). We use these preliminary results in our analysis of cluster weightings in §3.3.

### 3. COMPARATIVE ANALYSIS

#### 3.1. qLMXB Spatial Distribution

Grindlay et al. (1984) estimated the typical mass of the bright LMXBs in eight globular clusters by analyzing the distribution of the radial offsets of these sources relative to the cluster centers. This approach assumes that the sources have a common mass and that the cluster potentials have a common structure. It is also assumed that the distributions of X-ray sources and normal stars are in thermal equilibrium. In this case, the most massive group of normal stars is expected to be approximately distributed as a King (1966) model. This analysis results in an estimate for the ratio  $q = M_X/M_*$  of the source mass to the mass of the typical star that defines the optical core radius. Using a maximum likelihood analysis, Grindlay et al. (1984) found a most likely value of  $q = 2.6$  with a 90% confidence range of  $1.8 - 3.8$ . In this section, we adapt this analysis to the qLMXB distribution, in order to estimate the qLMXB mass.

Grindlay et al. (2002) describe a maximum-likelihood approach for fitting “generalized King models” to the projected radial distributions of cluster objects. In this model, the projected surface density of each component is described by,

$$S(r) = S_0 \left[ 1 + \left( \frac{r}{r_0} \right)^2 \right]^{\alpha/2}, \quad (1)$$

where  $\alpha$  is the power-law index and the core radius  $r_c$  is related to the radial-scale parameter  $r_0$  by  $r_c = (2^{-2/\alpha} - 1)^{1/2} r_0$ . Grindlay et al. (2002) obtained independent estimates of  $r_c$  and  $\alpha$  for various source populations in 47 Tuc by maximum likelihood fits of Eqn. (1). If the optical core radius  $r_{c*}$  of the cluster is defined by stars of mass  $M_*$  that have a standard King-model distribution ( $\alpha_* = -2$ ), then the core radius and slope for the distribution of sources of mass  $M_X = qM_*$  are related to  $q$  by,

$$r_{cX} = \left( 2^{2/(3q-1)} - 1 \right)^{1/2} r_{c*} \quad (2a)$$

$$\alpha_X = 1 - 3q \quad (2b)$$

In the present study, we first explored two-parameter maximum-likelihood fits of Eqn. (1) to the distribution of 20 qLMXBs in seven clusters with King-model structure (47 Tuc, NGC 6440, Terzan 5, M80, M28,  $\omega$  Cen, and M13—note that we include the Terzan 5 transient LMXB). However, this produced large uncertainty ranges for both  $r_{cX}$  and  $\alpha_X$ , and thus did not provide much useful information on the qLMXB mass. We then performed

single-parameter fits by determining the value of  $q$  that maximizes the likelihood of observing the given sample, with  $r_{cX}$  and  $\alpha_X$  given by Eqn. (2). Thus, we fit the function,

$$S(r) = S_0 \left[ 1 + \left( \frac{r}{r_{c*}} \right)^2 \right]^{(1-3q)/2}. \quad (3)$$

This is similar to the approach of Grindlay et al. (1984). We estimate the uncertainty range for  $q$  by fitting 1000 bootstrapped resamples of the original 20-source sample (see Cohn et al. 2002). The result is  $q = 1.9 \pm 0.2$  ( $1-\sigma$ ) with a 90% confidence range of  $1.6 \leq q \leq 2.2$ . The corresponding values of core radius and slope are  $r_{cX} = (0.60 \pm 0.04) r_{c*}$  and  $\alpha_X = -4.5 \pm 0.5$ .

We note that the assumption of thermal equilibrium among the cluster objects is not strictly justified for  $\omega$  Centauri, which has not reached equipartition (Anderson, 1997). Therefore, we removed the qLMXB in  $\omega$  Cen from our sample and repeated the analysis, and derived the same results. We performed the same analysis upon the sample of eight LMXBs used in Grindlay et al. (1984), finding  $q = 2.2$  with 90% confidence range of  $1.7 \leq q \leq 3.7$ . This is in reasonable agreement with their determination of  $q = 2.6$ ,  $1.8 \leq q \leq 3.8$  (90% confidence), with the major difference being that the current analysis does not consider offset measurement errors (negligible for *Chandra* positions). Finally, we performed the same analysis upon the sample of soft X-ray sources in 47 Tuc from Grindlay et al. (2002), differing from that analysis by parameterizing both the core radius and power-law slope  $\alpha$  in terms of a single  $q$ . Our new value for these soft sources is  $q = 1.58 \pm 0.13$ , 90% confidence range  $1.40 \leq q \leq 1.81$ .

If we assume that the optical profiles of the sample clusters, from which the core radii were determined, are dominated by turnoff-mass objects, then a reasonable estimate for  $M_*$  is  $0.8 M_\odot$  (see, e.g., King et al. 1998). This results in a most-likely qLMXB mass of  $M_X = (1.5 \pm 0.2) M_\odot$  with a 90% confidence range of  $1.3 M_\odot \leq M_X \leq 1.8 M_\odot$ . This range comfortably allows for a Chandrasekhar-mass neutron star with a low-mass companion. For the soft sources in 47 Tuc (which probably include some ABs as well as MSPs, Edmonds et al. 2003b), we derive a mass range of  $M_X = 1.26 \pm 0.10 M_\odot$ , 90% confidence range  $1.12 M_\odot \leq M_X \leq 1.45 M_\odot$ . For the eight LMXBs from Grindlay et al. (1984), our 90% confidence range is  $1.4 M_\odot \leq M_X \leq 3.0 M_\odot$ . Both of these estimates are also consistent with the qLMXB range.

#### 3.2. Luminosity Functions

Recent work by Pooley and collaborators (Pooley et al. 2002b, 2003a) has shown clear differences between luminosity functions (LFs) of different clusters, attributed in large part to differences in source makeup (e.g. large numbers of MSPs and ABs in 47 Tuc compared to NGC 6397). The LFs of globular cluster X-ray sources should be affected both by the relative numbers of different sources in each cluster, and by the properties of the individual populations. Here we make a first attempt to characterize the LFs for two identifiable source populations, qLMXBs and harder sources with  $L_X > 10^{31}$  ergs s $^{-1}$ , identified as mostly CVs (see §2). For the latter group, we test whether the hard source luminosity functions in different clusters

are consistent, in order to identify possible differences between the CV populations of different clusters.

To study the luminosity distributions of these populations, we follow the formalism of Johnston & Verbunt (1996), and Pooley et al. (2002a). Due to the relatively small numbers of sources, we assume for this analysis a simple power-law shape for the LF above a limiting luminosity. We derive the best-fit luminosity function by forming the quantities  $z_j = (L_j^i/L_i)^{-\gamma}$  and finding the  $\gamma$  that most uniformly distributes the  $z_j$  along the interval [0,1]. Here  $L_i$  is the limiting luminosity to which the cluster has been searched, or the minimum luminosity of the analysis. If the true LF is not a power-law, using differing limiting luminosities for different clusters will generate apparent differences between LFs of different clusters. Therefore we attempt to use the same limiting luminosity for each cluster within one analysis. For qLMXBs we include all qLMXBs in §2, analyzing both the luminosities generated with 10 km fits and those where the radius was allowed to float. We take as our minimum luminosity the lowest luminosity of a detected qLMXB. This leaves only Terzan 5 with a higher limiting luminosity, as we could detect qLMXBs with lower luminosities in each of the other clusters. We perform our qLMXB analysis both with and without the (lower S/N) Terzan 5 data, using the faintest qLMXB detected in Terzan 5 as its limiting luminosity. The results of this analysis are listed in Table 3, and the cumulative qLMXB luminosity function for all clusters except Terzan 5 is shown in Figure 2.

For the harder, primarily CV sources above  $10^{31}$  ergs  $s^{-1}$ , we use the luminosities reported in GHE01a for 47 Tuc, in Pooley et al. (2002a) for NGC 6752, and in Heinke et al. (2003c) for M80. For NGC 6397, we have adjusted the luminosities calculated in GHE01b for a distance of 2.7 kpc (Anthony-Twarog & Twarog 2000). For M28, we calculated the 0.5-2.5 keV unabsorbed X-ray luminosities of sources within the half-mass radius of the cluster from the reported 0.5-8.0 keV fits using PIMMS and the spectral fits in Becker et al. (2003). We use the MEKAL fits reported for M28 sources 17, 25, and 28, and the power-law fit for the remaining 11 sources (excluding the MSP). We have not removed the five known active binaries from this distribution, but we have removed the bright MSP in M28. We have not subtracted possible background AGN, which should number no more than 1-2 among these sources. We show the cumulative LF for the hard sources in these five clusters in Figure 2, along with the LFs for the hard sources in 47 Tuc and NGC 6397 separately. We also analyze the combined LF above  $5 \times 10^{31}$  ergs  $s^{-1}$  for these five clusters plus NGC 6440 (Pooley et al. 2002a), which suffers incompleteness and crowding at lower luminosities. Finally, we separately analyze the hard source LFs down to  $10^{31}$  ergs  $s^{-1}$  for the five deep cluster observations (47 Tuc, NGC 6397, NGC 6752, M80, and M28). The results of these analyses are listed in Table 3, while some of the KS probabilities as a function of  $\gamma$  are shown in Figure 3.

The index of the qLMXB luminosity function depends strongly upon the chosen minimum luminosity. Assuming the qLMXBs are 10 km objects, the best-fit X-ray luminosity slope above the minimum is  $\gamma = 0.6$ , while the bolometric luminosity slope is slightly steeper. The LFs of the hard source population in NGC 6397 and 47 Tuc

are clearly distinct, and that of NGC 6397 differs from the other globular clusters in general (Figures 2 and 3). Since CVs make up most of these hard sources, there must be a difference in the CV properties between these clusters. (Removing the three known ABs among the 47 Tuc sources and the one known AB among the 6397 sources does not affect the results.) We note that several cluster properties appear to correlate with the slope of the hard source LFs; cluster central density (inverse correlation), cluster metallicity, and cluster collision frequency  $\Gamma$  (see Table 1). Since a large part of these correlations are due to the unusual cluster NGC 6397 (see §4.3, 4.4), we do not attempt to draw conclusions about which properties are responsible for the different LF slopes.

Possible high-luminosity cutoffs may exist in the luminosity functions for both CVs and qLMXBs, as seen in Figure 2. We judge these cutoffs to be at roughly  $L_X(0.5-2.5 \text{ keV}) = 2 \times 10^{32}$  ergs  $s^{-1}$  for the CVs, and  $10^{33}$  ergs  $s^{-1}$  for the qLMXBs. KS tests show both samples to be formally consistent with power-laws with no high- $L_X$  cutoffs. However, the KS probability decreases and  $\gamma$  increases as the limiting luminosity increases, suggesting a cutoff. As the number of globular cluster X-ray sources identified in these luminosity ranges increases, it will become worthwhile to fit more complicated luminosity functions to the data.

### 3.3. Dependence of X-ray Source Numbers upon Cluster Density and Core Radius

We use the numbers of qLMXBs in several clusters of different structural parameters (all the clusters from Table 1) to attempt to constrain qLMXB and CV formation mechanisms. We assume that dynamical formation of globular cluster X-ray sources can be parametrized as  $\Gamma = \rho_c^\alpha r_c^\beta$ , where  $\Gamma$  is the formation rate,  $\rho_c$  is the central luminosity density, and  $r_c$  is the core radius. We follow the density weighting method of Johnston & Verbunt (1996) to test the dependencies of qLMXB formation upon the exponents  $\alpha$  and  $\beta$ . This method calculates the weight for each cluster based upon the choice of  $\alpha$  and  $\beta$ , and assigns a line length proportional to that weight. The line length is reduced by the fraction of X-ray sources to our chosen limit that are detectable in each cluster. This only affects Terzan 5; using the estimate of 30% incompleteness above  $10^{32}$  ergs  $s^{-1}$  (due to the LMXB, Heinke et al. 2003b), we find that 70% of the qLMXBs in Terzan 5 should have been detected, or 85% if the transient is included. The X-ray sources within each cluster are spread evenly along the line segment, and then the clusters are ordered by increasing weight to form a line of unit length with all the X-ray sources spread along it. A KS test then is applied to check whether the sources are consistent with a uniform distribution. The results of KS tests for a range of values of  $\alpha$  and  $\beta$  are shown in Figure 4, with the best-fit combination marked with a cross and 90%, 50%, and 10% KS probability contours marked. The meaning of a KS probability P is that a random distribution will be less uniform than the data P% of the time. However, since we distribute the sources evenly within each line segment, the KS probabilities will be overestimates. Although the results are not extremely constraining, clearly  $\alpha$  is best fit near a value of 1.5.

We perform the same analysis for harder sources above  $10^{31}$  ergs  $s^{-1}$  in a few clusters, which we believe are largely CVs, and the subset of those sources above  $10^{32}$  ergs  $s^{-1}$  in a larger range of clusters. To avoid dependence of our results upon the assumed LF, we use data that are complete to our chosen limiting luminosity except for Terzan 5, where the incompleteness to  $10^{32}$  ergs  $s^{-1}$  is 30%. For hard sources above  $10^{32}$  ergs  $s^{-1}$ , we use all the clusters in Table 1 except NGC 6366 (for which cluster membership is in doubt for all sources). For hard sources above  $10^{31}$  ergs  $s^{-1}$ , we exclude Terzan 5, NGC 6440, M13, and NGC 6366 due to their incompleteness. For  $\omega$  Cen the results of Cool et al. (2002) and Gendre et al. (2003a) are in close agreement on the numbers of X-ray sources above  $10^{31}$  ergs  $s^{-1}$  within the half-mass radius (15 vs. 16; source # 9 brightened in the XMM data). This sample includes only one soft source, the qLMXB, so foreground stars do not seem to be a problem. We estimate 4.7 background AGN from the analysis of Giacconi et al. (2001), and so estimate 9 hard sources above  $10^{31}$  ergs  $s^{-1}$  belong to the cluster (at the time of the *Chandra* observation). We also subtract one expected background source from NGC 6266 and M28, and two expected background sources from 47 Tuc and NGC 5904, producing the numbers listed under Hard Srcs in Table 1.

The results of these tests are shown in Figures 5 and 6, for the bright and full sample of hard sources, respectively. The hard sources require lower values of  $\alpha$  than the qLMXBs, and the sources above  $10^{31}$  ergs  $s^{-1}$  seem to require values of  $\beta$  less than 2. This reduced dependence on the core radius may be traced to the large number of CVs in NGC 6397, which is a core-collapsed cluster with a very small core radius. We repeat the test for the full sample of hard sources excluding NGC 6397, and find  $\beta$  to be much more loosely constrained (Figure 7). We discuss these results in §4.3.

#### 4. DISCUSSION

##### 4.1. Spatial distribution, spectra and variability

The spatial distribution of our qLMXB sample agrees with our expectation that these objects have masses characteristic of NSs plus low-mass companions. The implied average qLMXB system mass of  $1.5_{-0.2}^{+0.3}$  (90% conf. errors)  $M_{\odot}$  indicates that most NSs in qLMXBs have not accreted  $\sim 0.5 M_{\odot}$  from their companions. This is in general agreement with estimates of the masses of persistent LMXBs in several globular clusters ( $1.8_{-0.4}^{+1.2} M_{\odot}$ , Grindlay et al. 1984 recalculated in §3.1) and possible MSPs in 47 Tuc, thought to be their descendants ( $1.26_{-0.19}^{+0.14} M_{\odot}$ , Grindlay et al. 2002 recalculated in §3.1), both derived using the same method. It is also in agreement with the masses of pulsars (and MSPs in particular) derived by Thorsett & Chakrabarty (1999),  $1.35 \pm 0.04 M_{\odot}$ , which indicates that very little mass is required to spin neutron stars up to millisecond periods. Although our finding does not rule out the possibility that some qLMXBs may have larger masses, it lends weight against the high mass interpretation of the bright qLMXB X7 in 47 Tuc (Heinke et al. 2003a). As massive neutron stars should cool faster than less massive ones (e.g. Colpi et al. 2001), the brightest qLMXB (X7) should not be the most massive one.

Most of the qLMXBs in Table 2 are consistent with a

$\sim 10$  km neutron star radius when fit with a hydrogen atmosphere model. A smaller radius might suggest that a polar cap was strongly heated, perhaps through ongoing accretion channeled by a magnetic field. A larger radius, as suggested for 47 Tuc X7 and M30 A1, can be explained by a more massive ( $> 1.7 M_{\odot}$ ) neutron star or by an alteration of opacity through continued accretion (see Heinke et al 2003a, Lugger et al. 2003). Either possibility is of great interest. We note that our method in this paper of calculating the errors on the radius of these qLMXBs underestimates the true errors (see in't Zand et al. 2001), and thus these radii should be taken only as a measure of consistency with expectations, and not as rigorous constraints. See Heinke et al. (2003a, & in prep.) and Lugger et al. (2003) for detailed constraints on the radius and/or mass of some of these qLMXBs.

The qLMXBs listed in Table 2 have very little or no power-law component, in contrast to field systems identified through their high-luminosity outbursts which require 10-40% of their 0.5-10 keV emission in this component. Some field qLMXBs that have recently been accreting (KS 1731-260, Wijnands et al. 2002b and refs therein; MXB 1659-298, Wijnands et al. 2003) allow a power-law component to constitute up to  $\sim 25\%$  of the 0.5-10 keV flux, but do not require it. The only globular cluster qLMXB to require this component, NGC 6440 CX1, is the only qLMXB among our sample to have experienced a recorded outburst. This gives additional support to the suggestion by Heinke et al. (2003a) that the strength of the power-law component may be a measure of continuing low-level accretion. We note that field qLMXBs that have shown intrinsic variability on short time scales (Cen X-4, Campana et al. 1997 and Rutledge et al. 2003; Aql X-1, Rutledge et al. 2002b) indicative of continued accretion clearly show this power-law component. However, M28 #26 shows variability on a timescale of months without evidence of this power-law component (Becker et al. 2003), which does not fit this paradigm. However, this variability may be due to changing  $N_H$  column depth. No qLMXB without a power-law spectral component has yet been shown to require variability in its thermal component, suggesting that the thermal emission in these systems is entirely due to deep crustal heating (Brown et al. 1998).

##### 4.2. Luminosity information

We use the theoretical scaling of qLMXB formation with central density and core radius (see §3.3, 4.3) to calculate relative  $\Gamma$ s for the clusters in Table 1, as percentages of the total formation rate in the galactic globular cluster system. We can extrapolate from the studied clusters to the remaining globular clusters in the catalog of Harris (1996), and thus estimate that roughly 95 accreting neutron star systems may be found among the entire galactic globular cluster system, in agreement with the estimate of Pooley et al. (2003b). As discussed in §4.5 below, unusual dynamical histories of some clusters may increase this number slightly. Thirty-eight accreting neutron star systems have now been identified (including the other eleven bright LMXBs and the qLMXB in NGC 6652). Seven times more qLMXBs in globular clusters are inferred than have been seen in outburst.

Wijnands et al. (2001, 2002a, 2003) suggest that there



exist a population of qLMXBs with long-duration outbursts ( $> 10$  years) and extremely long dormant periods (thousands of years). This is required to explain the low quiescent flux from several qLMXBs that have been accreting for many years, and thus would otherwise be expected to have very hot cores (Brown et al. 1998). Pfahl, Rappaport, & Podsiadlowski (2003) suggest that irradiation-induced mass transfer cycles, with long periods of dormancy, may be required to account for the apparent lack of LMXBs compared to the number of MSPs in the galaxy. Our evidence that most accreting neutron stars in globular clusters are in deep quiescence supports the picture of long dormant periods suggested by Wijnands, Pfahl and others, although globular cluster systems may be very different from field systems.

*Chandra* observations have been sufficiently sensitive to observe soft qLMXBs in many clusters below  $1 \times 10^{32}$  ergs  $s^{-1}$  (all clusters in Table 1 except Terzan 5, M13 and probably NGC 6440), but they have not been seen. Assuming 10 km radii in the spectral fits leads us to conclude that no bolometric (redshifted) luminosities are below  $2.3 \times 10^{32}$  ergs  $s^{-1}$ . This lower LF cutoff implies a lower limit to the time-averaged mass transfer rate of these systems in the Brown et al. (1998) model. If enhanced neutrino cooling is not active and the mass transfer is mostly conservative, the bolometric luminosity range of qLMXBs given in Table 2 translates to time-averaged mass transfer rates of  $3 \times 10^{-12}$  to  $7 \times 10^{-11} M_{\odot} \text{year}^{-1}$  (the latter for X7 in 47 Tuc).

This range may represent the actual mass transfer rates, or may be an underestimate due to enhanced neutrino cooling (e.g. Colpi et al. 2001) or nonconservative mass transfer. We note that the larger number is a factor of a few less than the disc stability criterion for systems of periods similar to X5 (8 hours) in 47 Tuc (King 2003). Significantly larger mass transfer rates would cause persistent emission instead of transient behavior. Taking these rates at face value, two explanations are plausible. Part of this range of mass transfer rates might be supplied by initially evolved secondaries, i.e. originally intermediate-mass X-ray binaries, as suggested to predominate by recent work (Pfahl et al. 2003). Alternatively, extremely old post-minimum systems will naturally generate low mass-transfer rates below  $10^{-11} M_{\odot} \text{year}^{-1}$  (King 2000). In this picture, the lower luminosity limit is attributed to the finite age of the systems, less than a Hubble time (L. Bildsten, 2003, priv. comm.). We note that this luminosity range can be taken as support for the Brown et al. (1998) deep crustal heating model. An even lower thermal luminosity has been observed from the (low mass-transfer,  $\dot{m} \sim 5 \times 10^{-12} M_{\odot} \text{year}^{-1}$ ) millisecond X-ray pulsar SAX J1808, and has been taken to imply enhanced neutrino cooling from the core (Campana et al. 2002). If such enhanced cooling is common among globular cluster qLMXB systems, the time-averaged mass transfer rates may be higher than we have calculated.

#### 4.3. Distribution among globular clusters

Several methods of production of globular cluster binary X-ray sources have been suggested. Normal evolution from primordial binaries is not a reasonable explanation for neutron star systems (Clark 1975), but may be able

to explain some CVs and ABs (Verbunt & Meylan 1988, Davies 1997). The numbers of such systems would depend upon the initial mass of the cluster and the primordial binary fraction, and would be suppressed by the destruction of wide binaries in close encounters (Davies 1997). Tidal capture of main-sequence stars by neutron stars or white dwarfs may generate large numbers of short-period systems (e.g. di Stefano & Rappaport 1994), while exchange encounters will tend to inject neutron stars into longer-period primordial binaries (e.g. Hut, Murphy & Verbunt 1991). Both of the latter mechanisms predict a rate of formation of neutron star binaries  $\Gamma$  proportional to  $\rho_c^2 r_c^3 / \sigma \propto \rho_c^{1.5} r_c^2$ , where  $\rho_c$  is the central luminosity density,  $r_c$  is the core radius, and  $\sigma$  the central velocity dispersion (Verbunt & Hut 1987, Verbunt 2003). This assumes that the mass-to-light ratio is similar in the cores of different globular clusters, and that most of the encounters happen within the core. The second assumption is a good approximation for King-model clusters due to the steep density decline outside the core, but is less accurate for core-collapsed clusters with a less steep decline outside the core. A more accurate calculation, as performed in Pooley et al. (2003b), integrates the density distribution out to large radii, using the best surface profiles available. Our method does allow us, however, to investigate the dependence of X-ray source formation on core density and core size separately.

Our simple method does not account for increased neutron star density in the core due to mass segregation (Verbunt & Meylan 1988), or for escape of neutron stars from globular cluster potential wells of different depth (see Pfahl et al. 2002). It also carries the potential for significant bias in that we only analyze a small sample of clusters, generally selected because of the existence of known X-ray sources and perhaps not representative of the general globular cluster system. With these caveats, we proceed.

Our test of the distribution of globular cluster neutron star systems in Figure 3 indeed shows compatibility with  $\Gamma \propto \rho_c^{1.5} r_c^2$ , as predicted by either tidal capture or exchange encounters. This result agrees with the results of Verbunt & Hut (1987) on bright cluster LMXBs and the simpler tests of Gendre et al. (2003b) and Pooley et al. (2003a, b) upon qLMXBs in globular clusters. We note that this result is also compatible with the results of Johnston, Kulkarni & Phinney (1992) on recycled pulsars (the products of accreting neutron star systems) and those of Johnston & Verbunt (1996) on globular cluster low-luminosity X-ray sources (the brightest of which are predominantly qLMXBs) when their neglect of the velocity dispersion  $\sigma \propto \rho_c^{0.5} r_c$  is considered (as noted in Verbunt 2003). Grindlay (1996), using measured velocity dispersions, indeed showed correlation of dim source numbers with the theoretical scaling.

For the harder sources (predominantly CVs), we do not find agreement with the theoretically predicted formation rate from close encounters. Figures 4, 5, and 6 show a weaker dependence upon the central density for hard sources than for qLMXBs. The density dependence of the hard sources is better fit by  $\Gamma \propto \rho_c^{\alpha} r_c^2$  with  $\alpha \sim 1.1-1.3$ , rather than  $\alpha \sim 1.5$  as for qLMXBs. One suggestion for the lower density dependence is that high density environments destroy CVs preferentially, possibly by encounters

with neutron stars (e.g. Pooley et al. 2002b, Verbunt 2003), especially during the core collapse process. NGC 6397, the densest globular cluster yet studied, has an apparent excess of X-ray sources (Table 1, and Pooley et al. 2003b), which suggests the opposite conclusion. However, NGC 6397 may be unusual for other reasons; see §4.4.

The formation of some CVs in globular clusters from primordial, undisturbed binaries (especially in massive, moderately dense clusters like  $\omega$  Cen; Davies 1997, Verbunt 2003) may partially explain the weaker dependence upon density. Many sources outside the half-mass radius of  $\omega$  Cen may be CVs, two of them brighter than  $L_X = 10^{32}$  ergs s $^{-1}$  (Cool et al. 2002, Gendre et al. 2003). Davies (1997) indeed predicts that CVs from primordial binaries should exist in the outer regions of this unrelaxed globular cluster. However, even if four bright primordial CVs exist in  $\omega$  Cen, the masses of the other globular clusters in Table 1 are so much smaller that most of their bright CVs must not be primordial. According to Pryor & Meylan (1993),  $\omega$  Cen is as massive as all the other globular clusters with bright CVs (except Ter 5 and NGC 6440) put together. These other clusters have 21 bright CVs, which shows that the majority of these CVs are not primordial.

#### 4.4. Other clusters and processes

Our analysis of X-ray source distributions is consistent with X-ray imaging studies of some dense high- $\Gamma$  clusters (Liller 1, Homer et al. 2001; M15, Hannikainen et al. 2003) which suggest numerous X-ray sources in the luminosity range of qLMXBs. However, several clusters with low predicted collision rates seem to have more X-ray sources than expected based on their structural parameters; besides NGC 6397, these include NGC 6712, NGC 288, NGC 6652, and Terzan 1. Other dynamical processes may be at work in these clusters.

Analysis of the core-collapse process suggests that binaries in the core release energy to passing stars by “hardening” into tighter orbits, thus slowing the collapse process before their ultimate ejection or merger (Hut et al. 1992, Fregeau et al. 2003). The hardening of binaries during core collapse might be expected to generate increased mass transfer rates and thus X-ray emission. As core collapse proceeds, main-sequence binaries will be destroyed, but neutron stars should be preferentially exchanged into binaries. The numbers of each kind of X-ray binary existing at any one time may thus be a function of the cluster dynamical history, as well as current structure. Differences in dynamical history may explain the unusually large numbers of CVs (and NS systems?) in NGC 6397 (see Table 1), compared to the similar core-collapsed globular clusters M30 and NGC 6544. The latter, while not yet surveyed by *Chandra*, has a ROSAT upper limit of  $L_X = 5.9 \times 10^{31}$  ergs s $^{-1}$  (Verbunt 2001) above which 5 sources exist in NGC 6397. NGC 6397 has recently been shown to be depleted in binaries compared to several other clusters (Cool & Bolton 2002), while it appears to have an abundance of X-ray sources. NGC 6397 also seems to show an unusually flat CV LF, compared to 47 Tuc and other clusters in general (§3.2, and Pooley et al. 2002b).

The cluster NGC 6712 (which contains a bright persistent ultracompact LMXB) shows evidence for multiple accreting binaries and blue stragglers despite its rel-

atively low density and  $\Gamma$  (Ferraro et al. 2000, Paltrinieri et al. 2001;  $\Gamma = 0.13$ ). The path of NGC 6712’s orbit through the galactic bulge suggests that it experiences strong tidal stripping from the galactic potential (Dauphine et al. 1996). NGC 6712’s declining mass function below the turnoff (de Marchi et al. 1999, Andreuzzi et al. 2001) gives strong evidence that it has been stripped of  $\geq 99\%$  of its initial mass (Takahashi & Portegies Zwart 2000). An analysis of the orbits and structure of 38 globular clusters by Dinescu, Girard & van Altena (1999) indicates that NGC 6712, NGC 6397, NGC 6121, NGC 288, Palomar 5, and possibly M80 have very high destruction rates. Ferraro et al. (2000) thus suggest that NGC 6712 is only the fossil remnant core of a once very massive cluster, heavily enriched in compact objects and binaries due to mass segregation. Disrupting globular clusters should be generally marked by an apparent excess of massive stars, binaries, and binary products (such as X-ray sources or blue stragglers), which will remain segregated in the core while the outer halo is stripped. This destruction process should deposit X-ray binaries from globular clusters into the galactic bulge (Grindlay 1985).

NGC 6652 and Terzan 1 each possess a bright LMXB, although their collision rates are very low ( $\Gamma = 0.18$  and 0.008 respectively). In addition, they are home to at least three and one additional X-ray sources above  $\sim 5 \times 10^{32}$  ergs s $^{-1}$ , respectively (Heinke et al. 2001; Wijnands et al. 2002a). The orbits of NGC 6652 and Terzan 1 have not yet been calculated, but Idiart et al. (2002) note that Terzan 1 seems to have captured metal-rich stars from the bulge, implying it was once much more massive. Two of NGC 6652’s X-ray sources, both probable neutron star systems, are well outside the core (Heinke et al. 2001). Although NGC 6652 does not show signs of core collapse, this implies an unusual dynamical state. Analysis of archival *HST* images to measure the stellar LF and surface profile of NGC 6652 could test this. NGC 6652 and Terzan 1 could be remnant cores of initially much more massive globular clusters on their way to destruction.

Several of the other high-destruction clusters show low-mass star depletion (NGC 6121, Kanatas et al. 1995; NGC 288, Bellazzini et al. 2002b; NGC 6397, Piotto, Cool & King 1997). Palomar 5 shows both low-mass star depletion (Grillmair & Smith 2001) and tidal tails (Odenkirchen et al. 2001). These facts suggest that cluster destruction processes may have concentrated these clusters’ X-ray populations as well, although not as severely as NGC 6712. Such processes have recently been suggested by Pooley et al. (2003b) to explain the apparent excess of X-ray sources in NGC 6397. Disentangling the effects of cluster destruction and core collapse on binary production will probably require significant theoretical work.

The very loose cluster NGC 288 has an X-ray source with  $L_X \sim 3 \times 10^{32}$  from ROSAT HRI data (Verbunt 2001), even though it is very poor with  $\Gamma=0.005$ . NGC 288 shows centrally concentrated binary stars and blue stragglers (Bellazzini et al. 2002a; Ferraro et al. 2003). However, Bellazzini et al. (2002a) think that it would be very difficult to re-expand NGC 288 to its current low density after compressing the core sufficiently to produce collisional products. They and Ferraro et al. (2003) instead suggest that NGC 288’s large numbers of blue stragglers

are the result of primordial binary evolution, like the halo blue stragglers in M3 (Ferraro et al. 1997), and may be due to an initially high binary fraction. The high destruction rate of NGC 288 suggests that its binary fraction may be enhanced by the removal of lower-mass single stars from the halo during its repeated disk shocks. It will be of great interest to see if the same processes that generate large numbers of blue stragglers in NGC 288 also produce numerous X-ray sources detectable in recent *Chandra* observations (principal investigator: W. G. H. Lewin).

Metallicity has been suggested to have an effect on the luminosity of extragalactic globular cluster X-ray sources (e.g. Kundu, Maccarone, & Zepf 2002). This metallicity effect may be due to differences in cluster initial mass functions (Grindlay 1993) or to the larger radii of metal-rich stars increasing both tidal capture and Roche-lobe overflow rates (Bellazzini et al. 1995). More massive clusters should be better able to retain neutron stars after their formation kicks (Pfahl et al. 2002), which will affect the numbers of MSPs as well as qLMXBs. Neither mass nor metallicity have obvious effects upon the galactic globular clusters studied here. Analyzing the effects of all the above factors on the various globular cluster populations will require deep observations of a number of clusters with very different parameters, paired with deep radio and optical datasets to clearly identify different source types below the luminosities discussed here.

## 5. CONCLUSIONS

We have created a catalog of known qLMXBs containing neutron stars in globular clusters, adding three probable qLMXBs in NGC 6440 to those already known. We have reanalyzed those qLMXBs in archived *Chandra* globular cluster observations using the hydrogen atmosphere models of Lloyd (2003), and find general consistency with 10 km radii. The hard power-law component required in the spectra of many field qLMXBs is absent in most globular cluster qLMXBs, with the notable exception of the recently active transient in NGC 6440. The radial distribution of these qLMXBs within their globular clusters is consistent with a mass of  $1.5^{+0.3}_{-0.2} M_{\odot}$ . This is as expected for accreting neutron star systems, and suggests that the neutron stars do not grow significantly in mass. Globular cluster qLMXBs range in luminosity from  $10^{32}$  ergs  $s^{-1}$  up to a few  $10^{33}$  ergs  $s^{-1}$ . Quiescent LMXBs below  $10^{32}$  ergs

$s^{-1}$  would have been identifiable in most clusters, so the cutoff implies a lower limit to the time-averaged mass accretion rate. This range of luminosities is consistent with the Brown et al. (1998) model for qLMXB emission, as higher mass transfer rates would lead to persistent systems and significantly lower rates would probably require systems older than a Hubble time.

The luminosity function of globular cluster qLMXBs is consistent with the LF of globular cluster sources analyzed by Johnston & Verbunt (1996), which is not surprising as they are usually the brightest sources in a cluster. The LFs of harder sources above  $10^{31}$  ergs  $s^{-1}$ , which are mostly CVs, appear to vary between clusters, suggesting an influence of metallicity or core collapse upon CV properties. The numbers of qLMXBs in different clusters are consistent with the relative numbers of close encounters, allowing either tidal capture or exchange encounters as a mode of production. This suggests that the total number of accreting neutron stars in globular clusters is near 100. The harder sources, however, show a lesser dependence upon density, suggesting that dense environments may tend to destroy CVs. The core collapse process could be responsible for differences in the numbers and types of X-ray binaries between NGC 6397 and similar clusters. Tidal destruction or evaporation of clusters may leave substantial numbers of X-ray sources in apparently poor clusters.

This study has begun to probe individual source populations across different globular clusters, and test the effects of varying central density and core radius upon the properties of two populations, qLMXBs and CVs. Future *Chandra* observations will allow us to test the effects of metallicity, cluster mass, and other dynamical processes in clusters. Deep optical and radio datasets are also allowing identification and study of populations of ABs and MSPs. In addition to understanding the properties of these binaries, this work offers an opportunity for a deeper understanding of globular cluster evolution.

We are very grateful to D. Pooley for communicating results of several globular cluster studies to us before publication. We also thank L. Bildsten for useful discussions, and A. Kong and D. Pooley for comments on the manuscript. C. O. H. acknowledges support from *Chandra* grant GO2-3059A.

## REFERENCES

- Anderson, A. J. 1997, Ph.D. Thesis, University of California, Berkeley  
 Andreuzzi, G., De Marchi, G., Ferraro, F. R., Paresce, F., Pulone, L., & Buonanno, R. 2001, *A&A*, 372, 851  
 Anthony-Twarog, B. J. & Twarog, B. A. 2000, *AJ*, 120, 3111  
 Arnaud, K. A. 1996, in G. Jacoby & J. Barnes, (eds.) *ASP Conf. Series Astronomical Data Analysis Software and Systems V.*, vol. 101, 17  
 Balucinska-Church & McCammon 1992, *ApJ* 400, 699  
 Bassa, C. et al. 2003 (in prep.)  
 Becker, W. et al. 2003, *ApJ* submitted (astro-ph/0211468)  
 Bellazzini, M., Pasquali, A., Federici, L., Ferraro, F. R., & Fusi Pecci, F. 1995, *ApJ*, 439, 687  
 Bellazzini, M., Fusi Pecci, F., Messineo, M., Monaco, L., & Rood, R. T. 2002a, *AJ*, 123, 1509  
 Bellazzini, M., Fusi Pecci, F., Montegriffo, P., Messineo, M., Monaco, L. & Rood, R. T. 2002b, *AJ* 123, 2541  
 Brown, E. F., Bildsten, L., & Rutledge, R. E. 1998, *ApJ* 504, L95  
 Campana, S., Mereghetti, S., Stella, L., & Colpi, M. 1997, *A&A* 324, 941  
 Campana, S., Colpi, M., Mereghetti, S., Stella, L., & Tavani, M. 1998, *A&ARv* 8, 279  
 Campana, S. et al. 2002, *ApJ*, 575, L15  
 Clark, G. W. 1975, *ApJ*, 199, L143  
 Cohn, H. N., Lugger, P. M., Grindlay, J. E., & Edmonds, P. D. 2002, *ApJ*, 571, 818  
 Colpi, M., Geppert, U., Page, D., & Possenti, A. 2001, *ApJ*, 548, L175  
 Cool, A. M., Grindlay, J. E., Cohn, H. N., Lugger, P. M., & Slavin, S. D. 1995, *ApJ*, 439, 695  
 Cool, A. M. & Bolton, A. S. 2002, *ASP Conf. Ser.* 263: *Stellar Collisions, Mergers and their Consequences*, 163  
 Cool, A. M., Haggard, D., Carlin, J. L. 2002, in F. van Leeuwen, J. D. Hughes, G. Piotto (eds.), *Omega Centauri, A Unique Window into Astrophysics*, Vol. 265 of *ASP Conference Series*, ASP, p. 277  
 D'Amico, N., Possenti, A., Fici, L., Manchester, R. N., Lyne, A. G., Camilo, F., & Sarkissian, J. 2002, *ApJ* 570, L89  
 Dauphole, B., Geffert, M., Colin, J., Ducourant, C., Odenkirchen, M., & Tucholke, H.-J. 1996, *A&A*, 313, 119  
 Davies, M. B. 1997, *MNRAS*, 288, 117

- de Marchi, G., Leibundgut, B., Paresce, F., & Pulone, L. 1999, *A&A*, 343, L9
- Dinescu, D. I., Girard, T. M., & van Altena, W. F. 1999, *AJ* 117, 1792
- Di Stefano, R. & Rappaport, S. 1994, *ApJ*, 423, 274
- Djorgovski, S. 1993, ASP Conf. Ser. 50: Structure and Dynamics of Globular Clusters, 373
- Edmonds, P. D., Gilliland, R. L., Heinke, C. O., Grindlay, J. E., & Camilo, F. 2001, *ApJ*, 557, L57
- Edmonds, P. D., Heinke, C. O., Grindlay, J. E. & Gilliland, R. L. 2002a, *ApJ*, 564, L17
- Edmonds, P. D., Gilliland, R. E., Camilo, F., Heinke, C. O., & Grindlay, J. E. 2002b, *ApJ*, 579, 741
- Edmonds, P. D., Gilliland, R. E., Heinke, C. O., & Grindlay, J. E. 2003a, *ApJ* submitted
- Edmonds, P. D., Gilliland, R. E., Heinke, C. O., & Grindlay, J. E. 2003b, *ApJ* submitted
- Ferraro, F. R. et al. 1997, *A&A*, 324, 915
- Ferraro, F. R., Paltrinieri, B., Paresce, F., & De Marchi, G. 2000 *ApJ*, 542, L29
- Ferraro, F. R., Possenti, A., D'Amico, N., & Sabbi, E. 2001, *ApJ*, 561, L93
- Ferraro, F. R., Sills, A., Rood, R. T., Paltrinieri, B., & Buonanno, R. 2003 *ApJ* in press (astro-ph/0301261)
- Fregeau, J. M., Gürkan, M. A., Joshi, K. J., & Rasio, F. A. 2003, *ApJ* submitted (astro-ph/0301521)
- Gehrels, N. 1986, *ApJ* 303, 336
- Gendre, B., Barret, D., & Webb, N. A. 2003a, *A&A*, 400, 521
- Gendre, B., Barret, D., & Webb, N. A. 2003b, *A&A* in press (astro-ph/0303471)
- Giacconi, R. et al. 2001, *ApJ* 551, 624
- Grillmair, C. J. & Smith, G. H. 2001, *AJ*, 122, 3231
- Grindlay, J. E., Hertz, P., Steiner, J. E., Murray, S. S., & Lightman, A. P. 1984, *ApJ*, 282, L13
- Grindlay, J. E. 1985, IAU Symp. 113, Dynamics of Star Clusters, 43
- Grindlay, J. E. 1993, ASP Conf. Ser. 48: The Globular Cluster-Galaxy Connection, 156
- Grindlay, J. E., Cool, A. M., Callanan, P. J., Bailyn, C. D., Cohn, H. N., & Lugger, P. M. 1995, *ApJ*, 455, L47
- Grindlay, J. E. 1996, in IAU Symp. 174, Dynamical Evolution of Star Clusters, ed. P. Hut & J. Makino (Dordrecht: Kluwer), 171
- Grindlay, J. E., Heinke, C. O., Edmonds, P. D., & Murray, S. S. 2001a, *Science* 292, 2290 (GHE01a)
- Grindlay, J. E., Heinke, C. O., Edmonds, P. D., Murray, S. S., & Cool, A. M. 2001b, *ApJ* 563, L53 (GHE01b)
- Grindlay, J. E., Camilo, F., Heinke, C. O., Edmonds, P. D., Cohn, H., & Lugger, P. 2002, *ApJ* 581, 470
- Hannikainen, D. C., Charles, P. A., van Zyl, L. & Kong, A. K. H. 2003, MNRAS submitted
- Harris, W. E. 1996, *AJ*, 112, 1487
- Heinke, C. O., Edmonds, P. D., Grindlay, J. E. 2001, *ApJ* 562, 363
- Heinke, C. O., Grindlay, J. E., Lloyd, D. A., & Edmonds, P. D. 2003a, *ApJ*, 588, 452
- Heinke, C. O., Edmonds, P. D., Grindlay, J. E., Lloyd, D. A., Cohn, H. N., & Lugger, P. M. 2003b, *ApJ* 590, in press (astro-ph/0303141)
- Heinke, C. O., Grindlay, J. E., Edmonds, P. D., Lloyd, D. A., Murray, S. S., Lugger, P. M. & Cohn, H. N., 2003c, *ApJ* submitted
- Hertz, P. & Grindlay, J. E. 1983, *ApJ*, 275, 105
- Homer, L., Deutsch, E. W., Anderson, S. F., & Margon, B. 2001, *AJ* 122, 2627
- Hut, P., Murphy, B. W., & Verbunt, F. 1991, *A&A*, 241, 137
- Hut, P. et al. 1992, *PASP*, 104, 981
- Idiart, T. P., Barbay, B., Perrin, M.-N., Ortolani, S., Bica, E., & Renzini, A. 2002, *A&A*, 381, 472
- in't Zand, J. J. M. et al. 1999, *A&A*, 345, 100
- in't Zand, J. J. M., van Kerkwijk, M. H., Pooley, D., Verbunt, F., Wijnands, R., & Lewin, W. H. G. 2001, *ApJ*, 563, L41
- Johnston, H. M., Kulkarni, S. R., & Phinney, E. S. 1992, in X-ray Binaries & Recycled Pulsars, ed. E. P. J. van den Heuvel & S. A. Rappaport (Dordrecht: Kluwer), 349
- Johnston, H. M. & Verbunt, F. 1996, *A&A* 312, 80
- Kanatas, I., Griffiths, W. K., Dickens, R. J., & Penny, A. J. 1995, *MNRAS*, 272, 265
- Katz, J. I. 1975, *Nature*, 253, 698
- King, I. R. 1966, *AJ*, 71, 64
- King, I. R., Anderson, J., Cool, A. M., & Piotto, G. 1998, *ApJ*, 492, L37
- King, A. R. 2000, *MNRAS*, 315, L33
- King, A. R. 2003, in Compact Stellar X-Ray Sources (astro-ph/0301118)
- Kundu, A., Maccarone, T. J., & Zepf, S. E. 2002, *ApJ*, 574, L5
- Liedahl, D. A., Osterheld, A. L., & Goldstein, W. H. 1995, *ApJ*, 438, L115
- Lloyd, D. A. 2003, *MNRAS* (submitted)
- Lugger, P. M., Cohn, H. N., & Grindlay, J. E. 1995, *ApJ*, 439, 191
- Lugger, P. M. et al. 2003 in prep
- Nowak, M. A., Heinz, S., & Begelman, M. C. 2002, *ApJ*, 573, 778
- Odenkirchen, M. et al. 2001, *ApJ*, 548, L165
- Paltrinieri, B., Ferraro, F. R., Paresce, F., & De Marchi, G. 2001, *AJ*, 121, 3114
- Pfahl, E., Rappaport, S., & Podsiadlowski, P. 2002, *ApJ*, 573, 283
- Pfahl, E., Rappaport, S., & Podsiadlowski, P. 2003, *ApJ* submitted (astro-ph/0303300)
- Piotto, G., Cool, A. M., & King, I. R. 1997, *AJ*, 113, 1345
- Pooley, D., et al. 2002a, *ApJ* 569, 405
- Pooley, D., et al. 2002b, *ApJ* 573, 184
- Pooley, D., et al. 2003a, in KITP Conference: *Globular Clusters: Formation, Evolution and the Role of Compact Objects* (Jan 27-31, 2003; [http://online.kitp.ucsb.edu/online/clusters\\_c03/](http://online.kitp.ucsb.edu/online/clusters_c03/))
- Pooley, D., et al. 2003b, *ApJ* submitted (astro-ph/0305003)
- Pryor, C. & Meylan, G. 1993, ASP Conf. Ser. 50: Structure and Dynamics of Globular Clusters, 357
- Rutledge, R. E., Bildsten, L., Brown, E. F., Pavlov, G. G., & Zavlin, V. E. 2001, *ApJ*, 551, 921
- Rutledge, R. E., Bildsten, L., Brown, E. F., Pavlov, G. G., & Zavlin, V. E. 2002a, *ApJ* 578, 405
- Rutledge, R. E., Bildsten, L., Brown, E. F., Pavlov, G. G., & Zavlin, V. E. 2002b, *ApJ* 577, 346
- Rutledge, R. E., Bildsten, L., Brown, E. F., Pavlov, G. G., & Zavlin, V. E. 2003, AAS/High Energy Astrophysics Division, 35, 42.03
- Sosin, C. A. 1997, Ph.D. Thesis, University of California, Berkeley
- Takahashi, K. & Portegies Zwart, S. F. 2000, *ApJ*, 535, 759
- Thorsett, S. E. & Chakrabarty, D. 1999, *ApJ*, 512, 288
- Van Leeuwen, F. & Le Poole, R. S. 2002, in ASP Conf. Ser.  *$\omega$  Centauri, a unique window in astrophysics*, ed. van Leeuwen, Piotto, Hughes
- Verbunt, F., Elson, R. & van Paradijs, J. 1984, *MNRAS* 210, 899
- Verbunt, F. & Hut, P. 1987, in IAU Symp. 125, Origin and Evolution of Neutron Stars, ed. D. J. Helfand & J.-H. Huang (Dordrecht:Reidel), 187
- Verbunt, F. & Meylan, G. 1988, *A&A*, 203, 297
- Verbunt, F. 2001, *A&A*, 368, 137
- Verbunt, F. 2003 in ASP Conf. Ser. *New Horizons in Globular Cluster Astronomy*, ed. Piotto, Meylan, Djorgovski, Riello (astro-ph/0210057)
- Webb, N. A., Gendre, B., & Barret, D. 2002, *A&A*, 381, 481
- Wijnands, R., Miller, J. M., Markwardt, C., Lewin, W. H. G., & van der Klis, M. 2001, *ApJ* 560, L159
- Wijnands, R., Heinke, C. O., Grindlay, J. E. 2002a, *ApJ* 572, 1002
- Wijnands, R., Guainazzi, M., van der Klis, M., Mendez, M. 2002b, *ApJ* 573, L45
- Wijnands, R., Nowak, M. Miller, J. M., Homan, J., Wachter, S., & Lewin, W. H. G. 2003, *ApJ* submitted (astro-ph/0207094)
- Zavlin, V. E., Pavlov, G. G., & Shibhanov, Yu. A. 1996 *A&A* 315, 141

TABLE 1  
Recent *Chandra* or XMM Globular Cluster Surveys

Cluster	$N_H$ ( $10^{22}$ cm $^{-2}$ )	D (kpc)	$\log(\rho_0)^a$ ( $L_\odot$ pc $^3$ )	$r_c$ (arcmin)	$\Gamma$ (% Gal.)	# NS	# Hard Srcs $^b$ ( $> 10^{32}$ )	( $> 10^{31}$ )	Ref.
NGC 6440	0.59	8.5	5.28	0.13	6.4	8	5	> 16	1, 2
Ter 5	1.20	8.7	5.23	0.13	5.9	>5	>4	?	3, 4
NGC 6266	0.26	6.9	5.14c?	0.18	5.2	5	5	26 $^b$	5, 6
47 Tuc	0.030	4.5	4.82	0.40	3.6	2	3	22 $^b$	7, 8
M80	0.094	10.3	4.87	0.11	1.7	2	3	14	9
M28	0.24	5.5	4.73	0.24	1.5	1	2	14 $^b$	10
NGC 6752	0.022	4.1	4.91c?	0.17	0.74	0	1	8	11, 3
$\omega$ Cen	0.09	5.3	3.03	3.15	0.64	1	2	$\sim 9^b$	12, 13, 14, 15
M30	0.017	9.8	5.04c	0.06	0.58	1	0	3	16
NGC 5904	0.017	7.5	3.91	0.42	0.48	0	0	4 $^b$	5
NGC 6397	0.10	2.7	5.41c	0.08	0.40	1	3	8	17, 18, 19
M22	0.22	3.2	3.64	1.42	0.39	0	0	3	20
M13	0.01	7.7	3.33	0.78	0.23	1	2	?	21, 22
NGC 6121	0.20	2.2	3.82	0.83	0.12	0	0	1	23, 5
NGC 6366	0.39	3.6	2.42	1.83	0.01	0	0-1	?	5, 21

Note. — Distances, reddening, core radius and cluster central density taken from the most recent X-ray analysis work, or from the Harris (1996) catalog (updated Feb. 2003) with a few updates. Central densities are recalculated from prescription of Djorgovski (1993). Numbers of sources from the quoted X-ray analyses inside the cluster half-mass radii, with luminosities in the 0.5-2.5 keV range. NS refers to all accreting neutron star systems, including transients in NGC 6440 and Terzan 5. Close encounter rate  $\Gamma$ , calculated by  $\Gamma \propto \rho_0^{1.5} r_c^2$ , as percentage of total galactic globular cluster system rate. References: (1) Pooley et al. 2002b, (2) this work, (3) Cohn et al. 2002, (4) Heinke et al. 2003b, (5) Pooley et al. 2003a, (6) Pooley et al. 2003c (in prep), (7) Grindlay et al. 2001a, (8) Heinke et al. in prep, (9) Heinke et al. 2003c, (10) Becker et al. 2003, (11) Pooley et al. 2002a, (12) Rutledge et al. 2002, (13) Cool et al. 2002, (14) Gendre et al. 2003a, (15) van Leeuwen & Le Poole 2002, (16) Lugger et al. 2003, (17) Grindlay et al. 2001b, (18) Anthony-Twarog & Twarog 2000, (19) Sosin 1997, (20) Webb et al. 2002, (21) Gendre et al. 2003b, (22) Verbunt 2001, (23) Bassa et al. 2003.

<sup>a</sup>c=core collapsed. NGC 6752 (Lugger et al. 1995.) and NGC 6266 (Harris 1996) may not be core-collapsed.

<sup>b</sup>Including subtraction of probable background sources, based on Giacconi et al. (2001) log N-log S. We have subtracted 1 hard source from NGC 6266, 2 from 47 Tuc, 1 from M28, 5 from  $\omega$  Cen, and 2 from NGC 5904.

TABLE 2  
Probable qLMXBs in Globular Clusters

Cluster, ID	Cts	Radius (km)	kT <sub>eff</sub> (eV)	N <sub>H</sub> (10 <sup>22</sup> cm <sup>-2</sup> )	χ <sub>ν</sub> <sup>2</sup> /dof	PL flux % (0.5-10 keV)	L <sup>∞</sup> , ergs s <sup>-1</sup> (0.5-2.5 keV)	(0.01-10 keV)	Ref.
47 Tuc, X5	4181	12.0 <sup>+7.5</sup> <sub>-3.5</sub>	119 <sup>+21</sup> <sub>-18</sub>	0.09 <sup>+0.05</sup> <sub>-0.05</sub>	1.38/26	0 <sup>+3</sup> <sub>-0</sub>	1.5 × 10 <sup>33</sup>	2.2 × 10 <sup>33</sup>	1, 2
47 Tuc, X7	5508	35 <sup>+22</sup> <sub>-12</sub>	84 <sup>+13</sup> <sub>-12</sub>	0.13 <sup>+0.06</sup> <sub>-0.04</sub>	1.20/26	0 <sup>+0.5</sup> <sub>-0</sub>	2.0 × 10 <sup>33</sup>	3.6 × 10 <sup>33</sup>	1, 2
ω Cen, #3	467	12.4 <sup>+3.9</sup> <sub>-3.1</sub>	77 <sup>+8</sup> <sub>-7</sub>	(0.09)	0.90/18	0 <sup>+12</sup> <sub>-0</sub>	1.9 ± .1(1.8) × 10 <sup>32</sup>	4.1(3.8) × 10 <sup>32</sup>	3, 12
6397, U24	660	10.0 ± 1.6	74 <sup>+7</sup> <sub>-6</sub>	(0.10)	0.88/23	0 <sup>+5</sup> <sub>-0</sub>	1.0 ± .03 × 10 <sup>32</sup>	2.3 × 10 <sup>32</sup>	4, 12
6440, CX1	247	5.9 <sup>+4.2</sup> <sub>-1.4</sub>	150 <sup>+31</sup> <sub>-19</sub>	(0.59)	0.47/10	28 <sup>+13</sup> <sub>-15</sub>	1.1 ± .1(1.3) × 10 <sup>33</sup>	1.4(1.6) × 10 <sup>33</sup>	5, 6, 12
6440, CX2	172	6.9 <sup>+6.4</sup> <sub>-2.4</sub>	137 <sup>+26</sup> <sub>-26</sub>	(0.59)	1.13/6	0 <sup>+19</sup> <sub>-0</sub>	9.0 ± .7(9.8) × 10 <sup>32</sup>	1.3(1.5) × 10 <sup>33</sup>	6, 12
6440, CX3	116	9.7 <sup>+12</sup> <sub>-1.7</sub>	108 <sup>+39</sup> <sub>-15</sub>	(0.59)	0.81/3	18 <sup>+16</sup> <sub>-17</sub>	6.6 ± .6 × 10 <sup>32</sup>	1.0 × 10 <sup>33</sup>	6, 12
6440, CX5	90	9.2 <sup>+0.2</sup> <sub>-4.4</sub>	109 <sup>+30</sup> <sub>-26</sub>	(0.59)	63%	5 <sup>+11</sup> <sub>-5</sub>	5.7 ± .6(5.9) × 10 <sup>32</sup>	9.0(9.4) × 10 <sup>32</sup>	6, 12
6440, CX7	43	3.6 <sup>+5.0</sup> <sub>-2.0</sub>	138 <sup>+58</sup> <sub>-38</sub>	(0.059)	49%	0 <sup>+15</sup> <sub>-0</sub>	2.1 ± .3(3.0) × 10 <sup>32</sup>	4.5(5.5) × 10 <sup>32</sup>	6, 12
6440, CX10	17	49 <sup>+178</sup> <sub>-20</sub>	48 <sup>+31</sup> <sub>-17</sub>	(0.59)	42%	0 <sup>+10</sup> <sub>-0</sub>	2.1 ± .5(1.3) × 10 <sup>32</sup>	9.4(2.9) × 10 <sup>32</sup>	6, 12
6440, CX12	12	6.8 <sup>+4.8</sup> <sub>-5.3</sub>	86 <sup>+69</sup> <sub>-44</sub>	(0.59)	50%	0 <sup>+42</sup> <sub>-0</sub>	9.0 ± 2.4(11.1) × 10 <sup>31</sup>	1.7(2.5) × 10 <sup>32</sup>	6, 12
6440, CX13	11	2.2 <sup>+20</sup> <sub>-0.8</sub>	127 <sup>+99</sup> <sub>-72</sub>	(0.59)	47%	0 <sup>+60</sup> <sub>-0</sub>	5.7 ± 1.6(10) × 10 <sup>31</sup>	8.6(23) × 10 <sup>31</sup>	6, 12
Ter 5, W2	37	3.1 <sup>+15</sup> <sub>-2.3</sub>	154 <sup>+118</sup> <sub>-73</sub>	(1.2)	0.63/5	0 <sup>+36</sup> <sub>-0</sub>	3.2 ± .8(4.5) × 10 <sup>32</sup>	4.3(7.8) × 10 <sup>32</sup>	7, 12
Ter 5, W3	77	1.6 <sup>+3.1</sup> <sub>-0.6</sub>	222 <sup>+50*</sup> <sub>-78</sub>	(1.2)	0.71/9	0 <sup>+53</sup> <sub>-0</sub>	4.0 ± .6(6.5) × 10 <sup>32</sup>	5.1(10.6) × 10 <sup>32</sup>	7, 12
Ter 5, W4	17	2.9 <sup>+280</sup> <sub>-1.1</sub>	143 <sup>+127*</sup> <sub>-115</sub>	(1.2)	1.49/11	-	2.1 ± .9(2.2) × 10 <sup>32</sup>	3.0(4.2) × 10 <sup>32</sup>	7, 12
Ter 5, W8	34	1.6 <sup>+280</sup> <sub>-1.1</sub>	189 <sup>+83*</sup> <sub>-132</sub>	(1.2)	0.43/6	3 <sup>+120</sup> <sub>-3</sub>	2.1 ± .7(3.6) × 10 <sup>32</sup>	3.0(6.4) × 10 <sup>32</sup>	7, 12
M28 #24	1669	11.1 <sup>+5.3</sup> <sub>-2.9</sub>	118 <sup>+39</sup> <sub>-14</sub>	0.26 ± 0.04	0.96/44	-	1.2 <sup>+7</sup> <sub>-4</sub> × 10 <sup>33</sup>	1.9 × 10 <sup>33</sup>	8
M13 Ga	-	9.8 ± 0.3	99 ± 4	0.11	0.55/15	-	4.3 ± .4 × 10 <sup>32</sup>	7.4 × 10 <sup>32</sup>	9
M30, A1	830	20.5 <sup>+22</sup> <sub>-5.7</sub>	86 <sup>+11</sup> <sub>-13</sub>	0.034 <sup>+0.055</sup> <sub>-0.018*</sub>	1.06/33	0 <sup>+6</sup> <sub>-0</sub>	8.8 ± .3 × 10 <sup>32</sup>	1.8 × 10 <sup>33</sup>	10
M80, CX2	227	9.3 <sup>+3.2</sup> <sub>-1.5</sub>	92 <sup>+13</sup> <sub>-10</sub>	(0.094)	1.12/8	0 <sup>+12</sup> <sub>-0</sub>	2.8 ± .2(2.8) × 10 <sup>32</sup>	5.1(5.2) × 10 <sup>32</sup>	11, 12
M80, CX6	62	4.2 <sup>+1.9</sup> <sub>-0.5</sub>	95 <sup>+22</sup> <sub>-4</sub>	(0.094)	50%	0 <sup>+22</sup> <sub>-0</sub>	8.0 ± 1.0(12.7) × 10 <sup>31</sup>	1.4(2.8) × 10 <sup>32</sup>	11, 12

Note. — Parameters derived from spectral fits to probable qLMXBs in globular clusters. Spectral fits in XSPEC, using models of Lloyd (2003; except for M28 and M13, see text) with grav. redshift fixed to 0.306 (except for 47 Tuc, M30; see refs). Photoelectric absorption fixed at the known galactic absorption to the cluster for the fainter sources, and equal or greater than the galactic absorption for brighter sources. Parameter values for CX5, CX7, CX10, CX12, CX13 in 6440 and CX6 in M80 derived using C statistic in XSPEC. For C statistic fits, the percentage of Monte-Carlo simulations generating a C statistic less than the best fit are given in place of the χ<sup>2</sup> statistic. Luminosities are given from the best fit and, where the fit is reasonable, for a fit with radius forced to 10 km (in parentheses). All errors are 90% confidence limits on one parameter, except for X-ray luminosity errors which are 1σ errors derived from counting statistics, ignoring uncertainty in other parameters. A \* indicates the fit encountered a hard limit. For M80 CX6, N<sub>H</sub> must be freed to allow an acceptable fit with radius=10 km, giving N<sub>H,22</sub> = 0.21<sup>+0.05</sup><sub>-0.10</sub>. References: (1) Grindlay et al. 2001a, (2) Heinke et al. 2003a, (3) Rutledge et al. 2002a, (4) Grindlay et al. 2001b, (5) Pooley et al. 2001b, (6) in't Zand et al. 2001, (7) Heinke et al. 2003b, (8) Becker et al. 2003, (9) Gendre, Barret, & Webb 2003, (10) Lugger et al. 2003 (in prep), (11) Heinke et al. 2003c, (12) re-analyzed in this work.

TABLE 3  
Luminosity Function Fits

Description	$L_{min}$	# srcs	$\gamma$	Prob
qLMXBs				
$L_X$ , R fixed	$1.0 \times 10^{32}$	17	$0.64^{+.31}_{-.22}$	81%
... with Ter 5	$1.0 \times 10^{32}$	21	$0.76^{+.36}_{-.30}$	90%
$L_X$ , R free	$5.7 \times 10^{31}$	17	$0.46^{+.15}_{-.10}$	49%
$L_{Bol}$ , R fixed	$2.3 \times 10^{32}$	17	$0.77^{+.43}_{-.29}$	91%
... with Ter 5	$2.3 \times 10^{32}$	21	$0.94^{+.48}_{-.41}$	93%
Harder Sources				
Only 47 Tuc	$1 \times 10^{31}$	18	$0.85^{+.61}_{-.37}$	99%
Only M80	$1 \times 10^{31}$	14	$0.65^{+.51}_{-.30}$	99%
Only M28	$1 \times 10^{31}$	14	$0.79^{+.64}_{-.24}$	66%
Only N6752	$1 \times 10^{31}$	8	$0.62^{+.57}_{-.27}$	85%
Only N6397	$1 \times 10^{31}$	8	$0.42^{+.29}_{-.13}$	54%
5 clusters	$1 \times 10^{31}$	62	$0.67^{+.20}_{-.12}$	80%
6 clusters	$5 \times 10^{31}$	25	$0.82^{+.19}_{-.15}$	42%

Note. — Results of KS tests for the LFs of source populations in several globular clusters. For qLMXBs, sources include those in Table 2 omitting the four Terzan 5 sources, except where indicated. For harder sources, the 5 clusters are those listed individually, with NGC 6440 added to study only the bright CVs (6 clusters).  $L_{min}$  is the limiting luminosity of each analysis (except for Terzan 5 qLMXBs, where  $L_{X,min} = 2 \times 10^{32}$  and  $4 \times 10^{32}$  ergs s<sup>-1</sup> for X-ray and bolometric luminosities).  $\gamma$  is the index of the best-fit LF ( $dN/dL_X \propto L_X^{-(\gamma+1)}$ ), and the listed errors are the range where the KS probability (Prob) is larger than 10% (where the KS probability is the probability that a random sample selected from the given distribution will have a larger statistic).

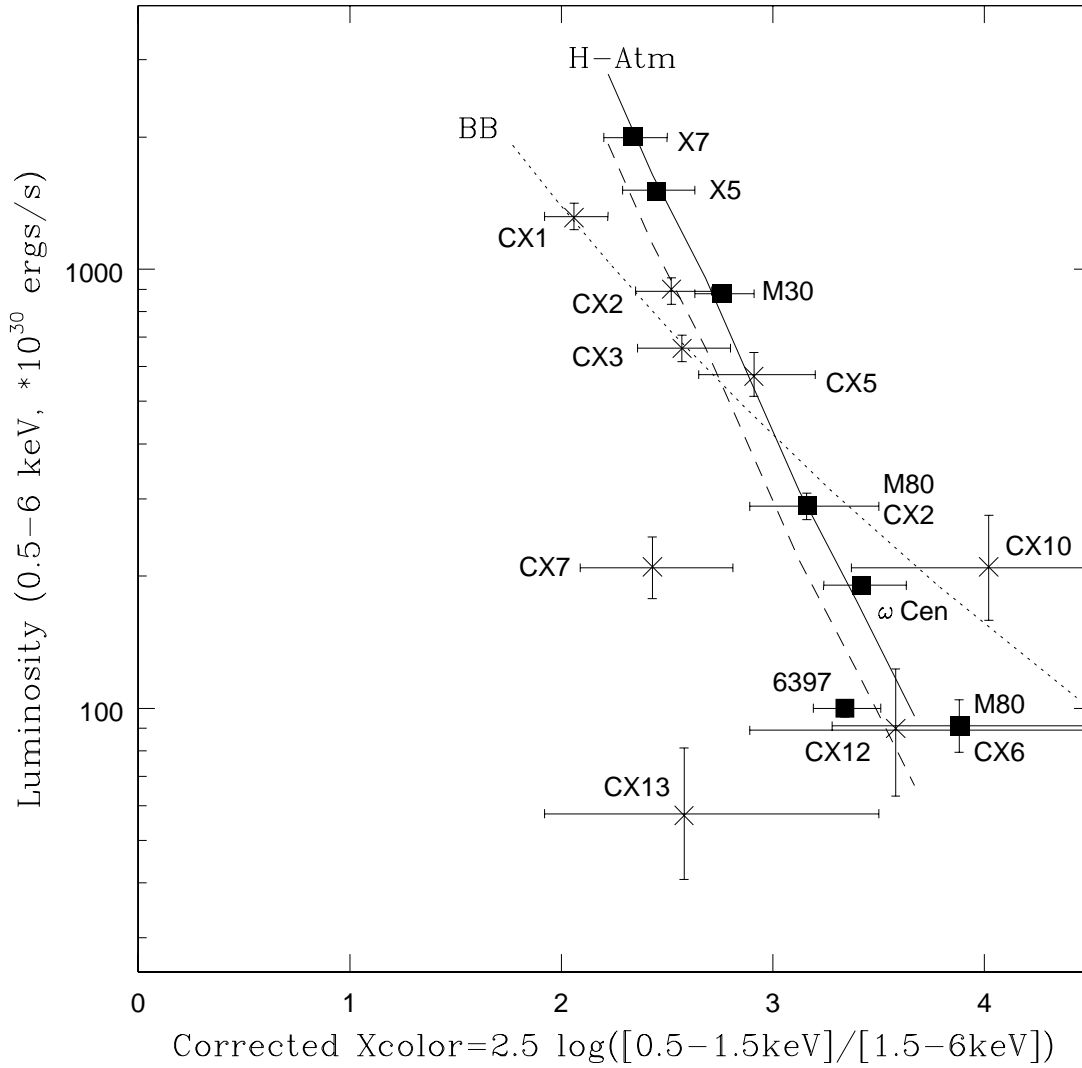


FIG. 1.— Standardized X-ray CMD with several qLMXBs and theoretical cooling tracks plotted. Crosses represent NGC 6440 probable qLMXBs, while squares represent qLMXBs from other clusters (NGC 6397,  $\omega$  Cen, M30, M80 CX2 and CX6, and 47 Tuc X5, X7). A theoretical 1.44 km blackbody track is plotted (dotted line), as are 10 (dashed) and 12 km (solid) nonmagnetic hydrogen-atmosphere models from Lloyd (2003). Errors are from Gehrels (1986) applied to the counts detected in each band, and do not include possible errors in the best-fit luminosity from spectral fitting. CVs (not shown) tend to have corrected Xcolors near zero on this scale.



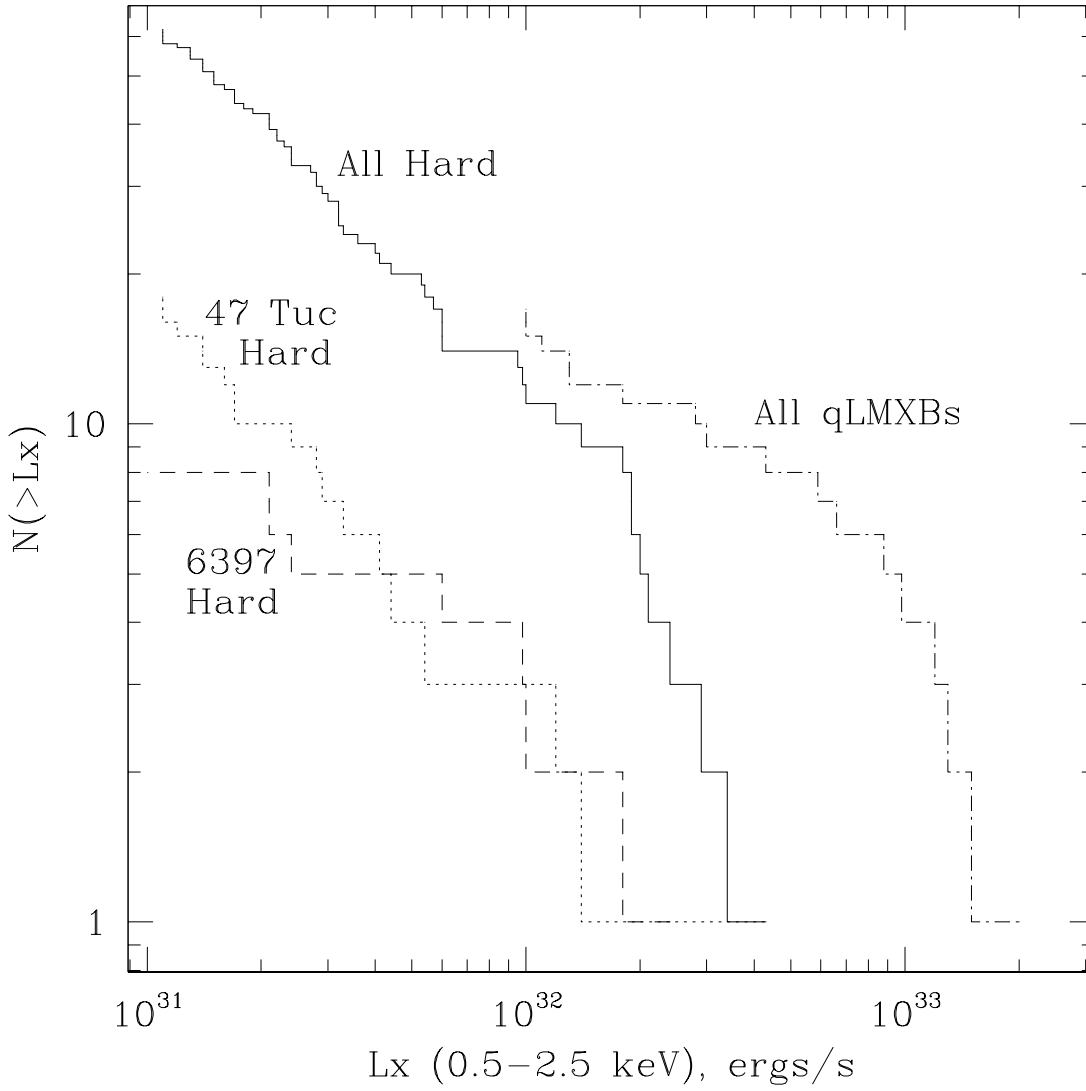


FIG. 2.— Cumulative luminosity functions of qLMXBs and probable CVs in globular clusters. The qLMXBs are from Table 2, using  $L_X$ s derived from fits assuming 10 km radius (where acceptable). The probable CVs are hard sources with  $10^{31} < L_X(0.5 - 2.5) < 10^{33} \text{ ergs s}^{-1}$ , with luminosities from 47 Tuc (GHE01a), NGC 6397 (GHE01b), NGC 6752 (Pooley et al. 2002a), M28 (Becker et al. 2002), and M80 (Heinke et al. 2003c). A few known active binaries have not been removed from the CV sample, but the bright MSP in M28 has been removed. One or two background AGN are also expected among these sources.

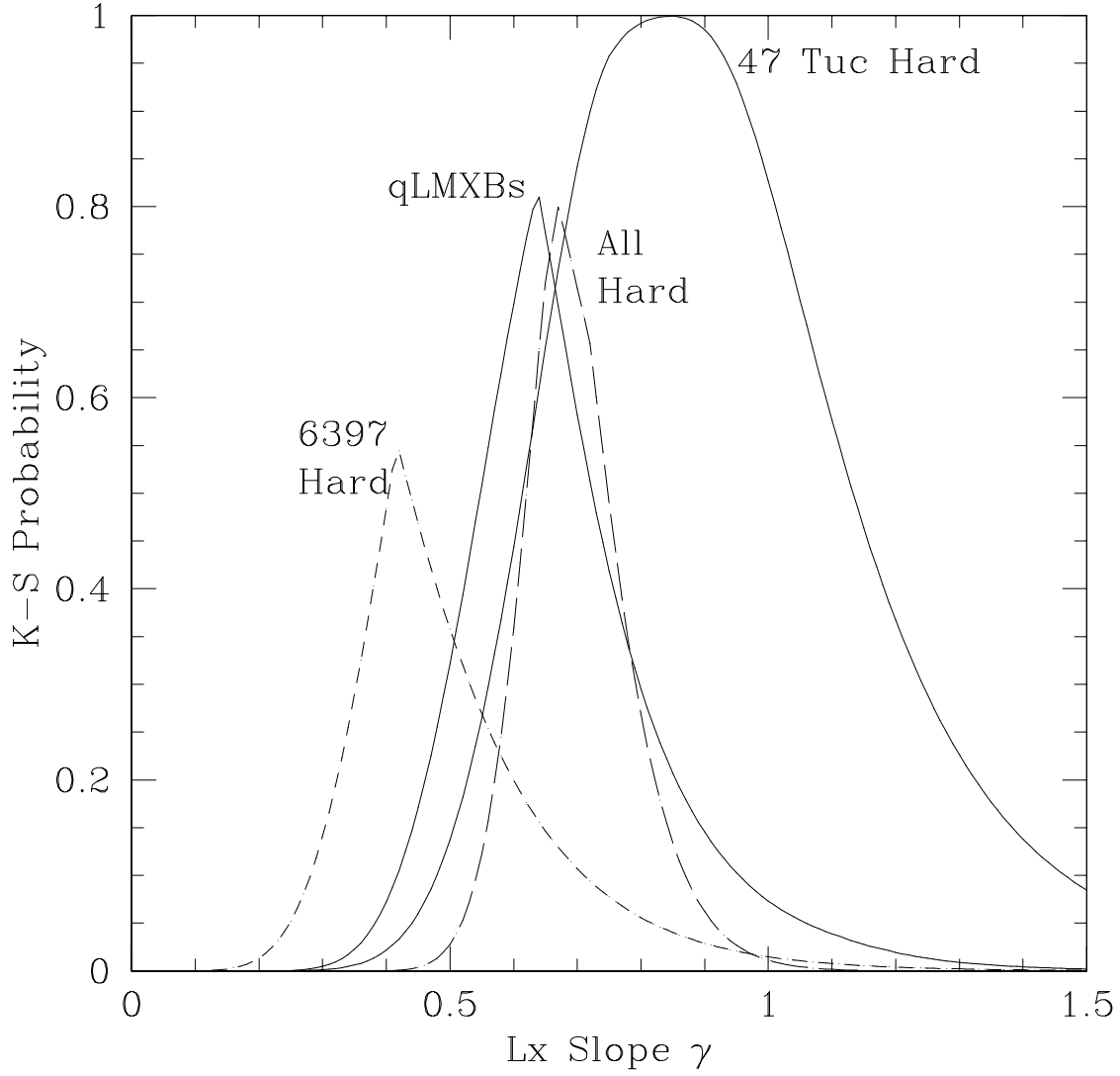


FIG. 3.— Comparison of the indices of power-law slopes for several different globular cluster populations. Kolmogorov-Smirnov probability is plotted as a function of  $\gamma$ , where the LF is assumed to be  $dN \propto L_X^{-\gamma} d \ln L_X$ . The qLMXB LF is that where qLMXB radii are assumed to be 10 km, and Terzan 5 qLMXBs are excluded (line 1 in Table 3).

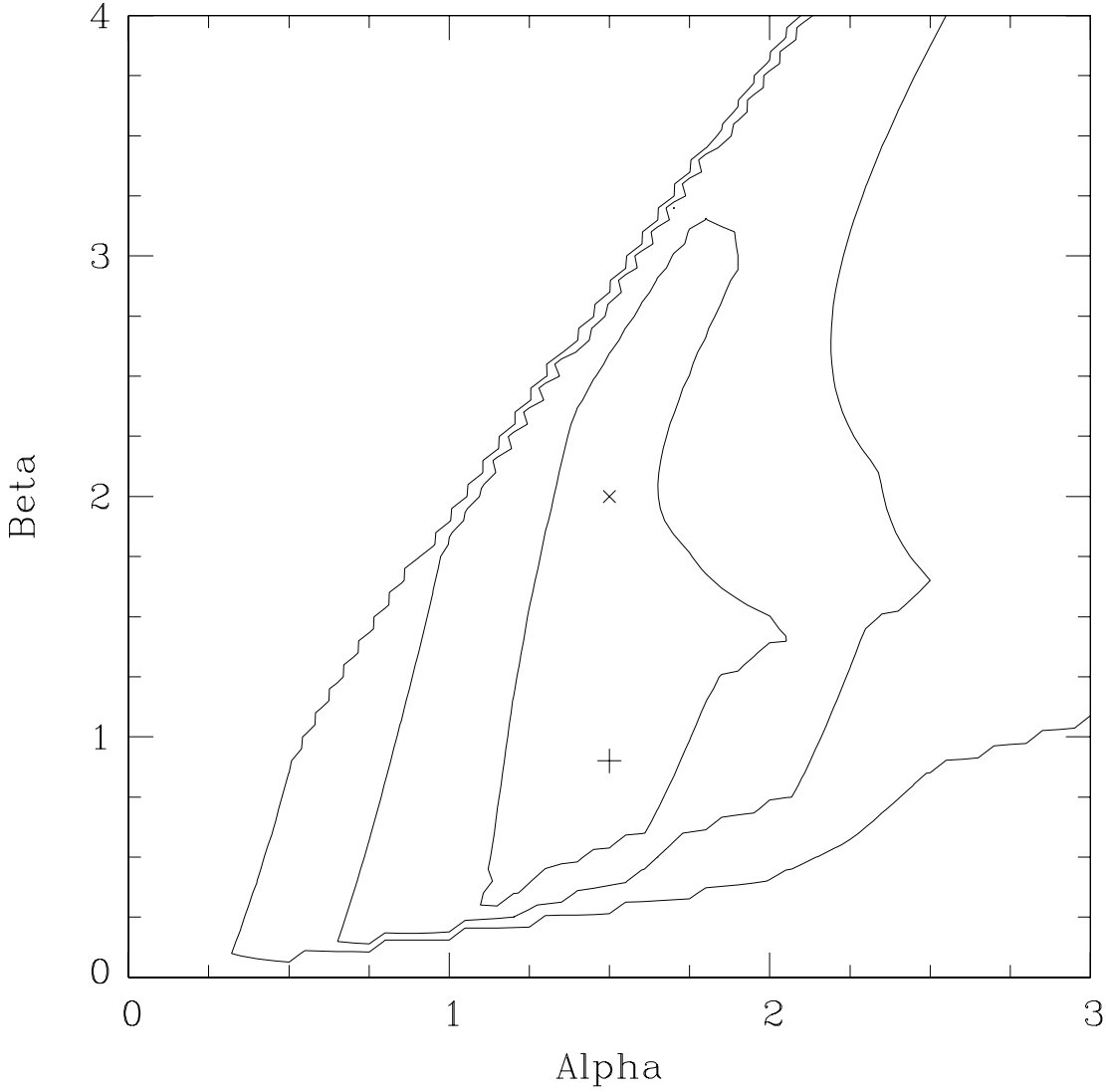


FIG. 4.— Kolmogorov-Smirnov probability contour map for the dependencies of qLMXB distribution among globular clusters upon central cluster density  $\rho_0$  and core radius  $r_c$ . The data are the numbers of accreting neutron stars (whether in outburst or quiescence) from all clusters in Table 1, plus an estimate of the incompleteness of the Terzan 5 survey (see text). We test the acceptability of a qLMXB formation rate  $\Gamma$  of the form  $\Gamma \propto \rho_0^\alpha r_c^\beta$  for various values of  $\alpha$  and  $\beta$ . Contours indicate K-S probabilities of an acceptable distribution of 10%, 50%, and 90%, while the cross (+) marks the best fit. The theoretically calculated close encounter rate dependency (Verbunt & Hut 1987) is indicated by an X.

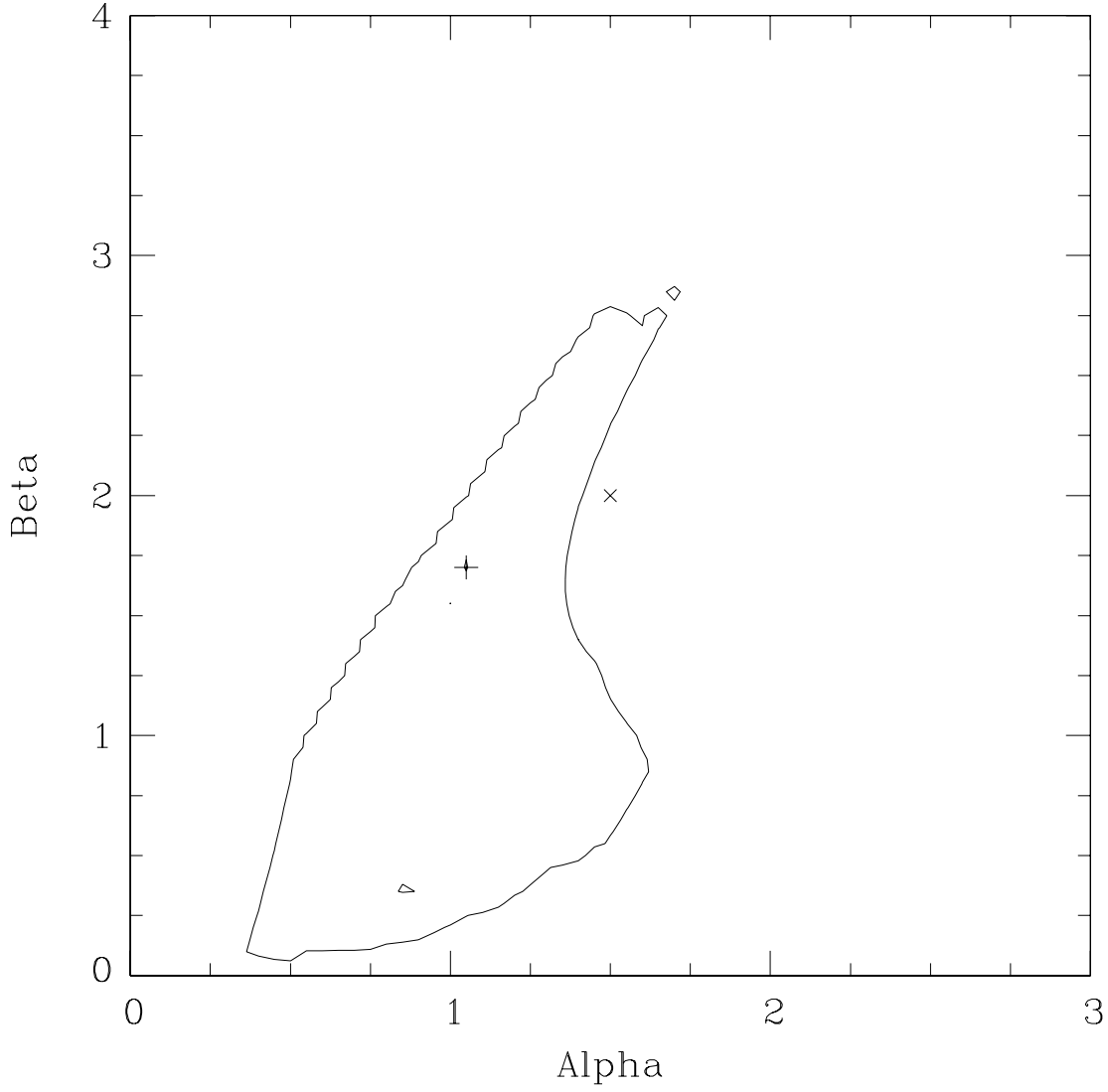


FIG. 5.— K-S probability contour map for the dependencies of hard globular cluster sources ( $10^{32} < L_X(0.5 - 2.5) < 10^{33}$  ergs  $s^{-1}$ ) upon  $\rho_0$  and  $r_c$ . Symbols and contours same as figure 4, except that no 90% contour is indicated. Data are bright hard sources from all clusters in Table 1 except NGC 6366 only.

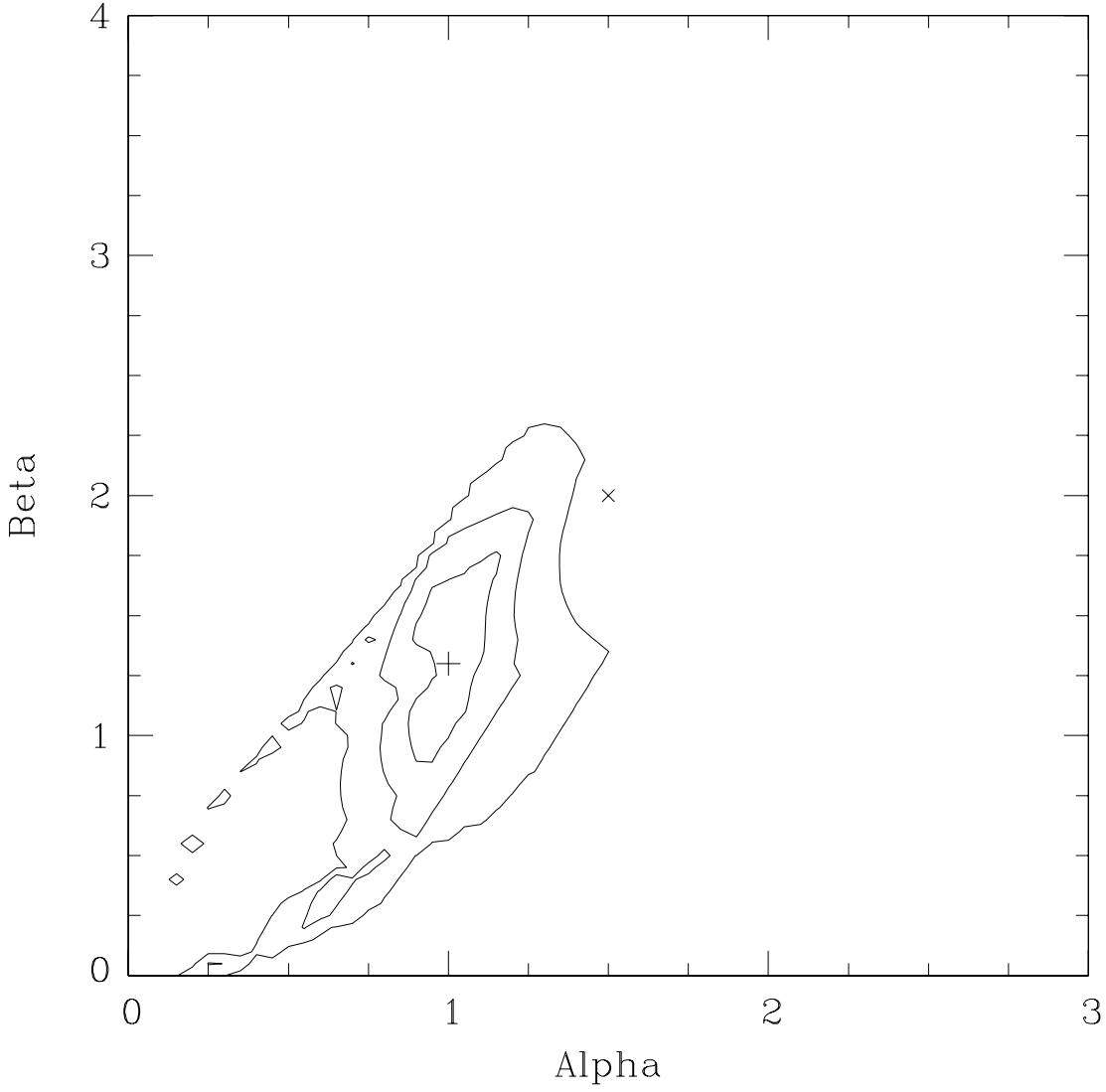


FIG. 6.— K-S probability contour map for the dependencies of hard globular cluster sources ( $10^{31} < L_X(0.5 - 2.5) < 10^{33}$  ergs  $s^{-1}$ ) upon  $\rho_0$  and  $r_c$ . Symbols and contours same as figure 4. Data are from Table 1, omitting Terzan 5, M13, NGC 6440, and NGC 6366.

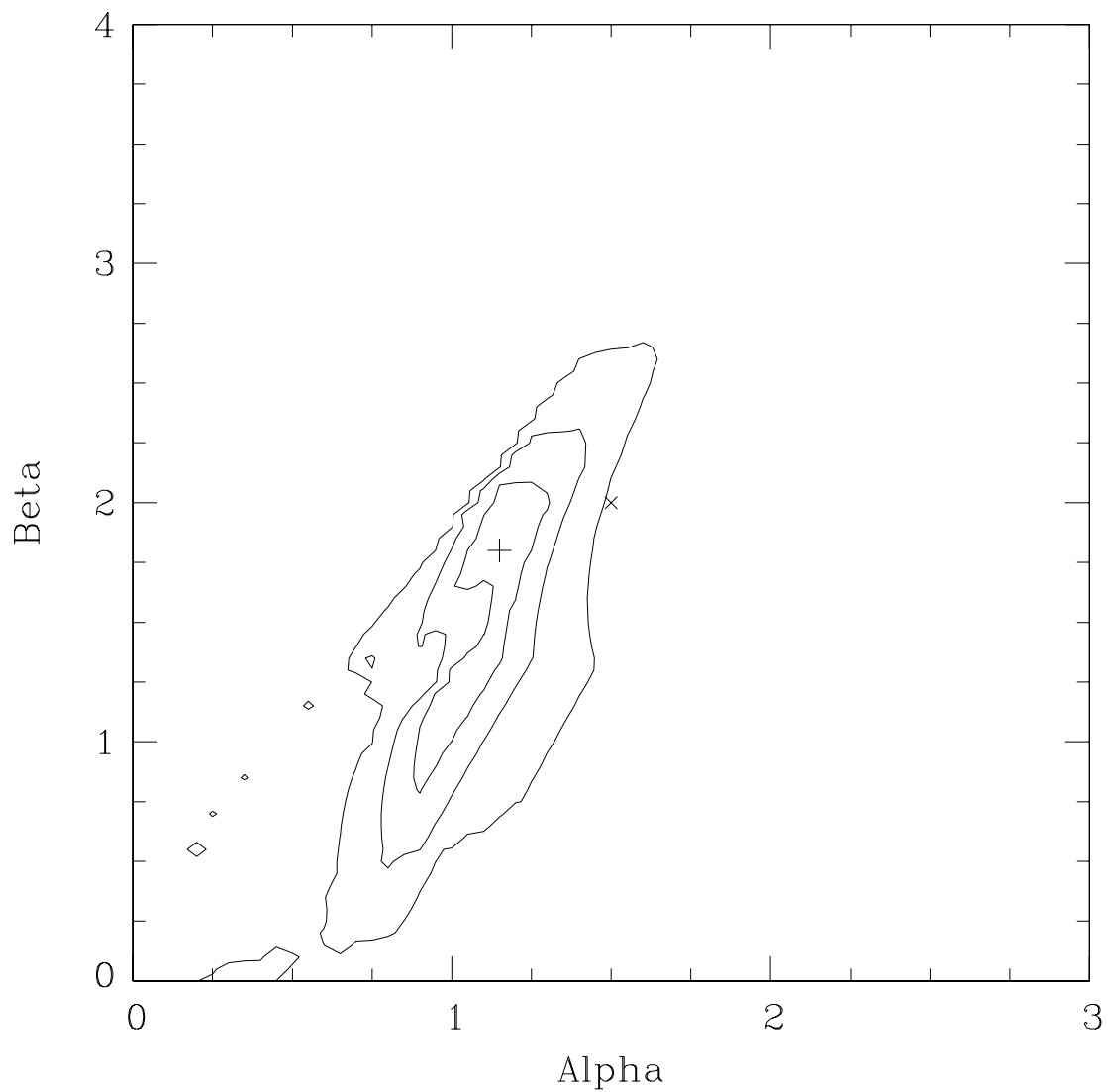


FIG. 7.— Same as figure 6, except that NGC 6397 is also excluded from the data.